EFFECTS OF μ-OPIOIDS ON NEURONS OF THE MEDIAL GENICULATE NUCLEUS

by

Takayo Ota

M.D., Kinki University, 1996

A THESIS SUBMITTED IN PARTIAL FULFILMENT OF

THE REQUIREMENTS FOR THE DEGREE OF

MASTER OF SCIENCE

in

THE FACULTY OF GRADUTE STUDIES

(Department of Pharmacology and Therapeutics)

We accept this thesis as conforming

to the required standard

THE UNIVERSITY OF BRITISH COLUMBIA

September, 2000

In presenting this thesis in partial fulfilment of the requirements for an advanced degree at the University of British Columbia, I agree that the Library shall make it freely available for reference and study. I further agree that permission for extensive copying of this thesis for scholarly purposes may be granted by the head of my department or by his or her representatives. It is understood that copying or publication of this thesis for financial gain shall not be allowed without my written permission.

Department of Pharmacology & Therapeutics

The University of British Columbia
Vancouver, Canada

Date Oct. 2, 00

DE-6 (2/88)

Abstract

Immunohistochemical and hybridization studies have revealed the presence of μ-, but not κ- and δ-opioid receptors in the medial geniculate body. Using whole-cell patch clamp techniques, I examined the effects of opioid agonists on gerbil MGB neurons (P9-P16) in vitro. The opioid effects were concentration-dependent. Opioids produced different actions on the input conductance (G_i) when applied in low, compared with high concentrations. The increase in G_i might be due to increase in K^+ conductance whereas the decrease in G_i might be due to I_H inactivation. When G_i was increased, the reversal potential was ~-65 mV; this implicates opioid actions on K^+, among other ion channels. In the case of decreased G_i, the opioid currents did not reverse from –100 mV to –50 mV, implying the involvement of cationic channels, other than K^+. DAMGO, a μ-selective opioid agonist, had a reversal potential that was similar to that observed when morphine increased G_i, implying that opioids activate μ-opioid receptors in MGB neurons. Tetrodotoxin altered the concentration-dependent action of morphine. Here, the suggestion is morphine's actions involve neurons that presynaptic to the patch clamped neuron. Morphine application blocked spike–frequency adaptation and reduced firing rates in response to depolarizing current pulse injection. Morphine application may block Ca^{2+}-mediated K^+ channels that inhibited spike-frequency adaptation. Such blockade may be expected to increase the spike frequency. However, the increased conductance due to morphine would shunt the Na^+ current, resulting in a lower spike frequency. The results of this study have revealed that opioids have both excitatory and inhibitory effects on MGB neurons.

Table of Contents

List of Figures

Tables

1. Introduction

In this thesis, I will describe my observations of the effects of opioids in the auditory thalamus of the central nervous system (CNS). These effects, while fascinating, remain somewhat enigmatic for straightforward interpretation. This is largely because a system dedicated to hearing is not known to mediate pain sensation. Nevertheless, several studies have demonstrated the existence of receptors for opioids in the auditory system and associated nuclei, specifically in the medial geniculate nucleus (MGB) of the thalamus and the central vestibular nucleus (Ding et al. 1996; Mansour et al. 1994; Sulaiman and Dutia 1998). Moreover, several groups have recently attempted to clarify the function of opioids in the auditory system. In the light of my observations, I will discuss near the end of the thesis, interpretations of the proposed functions and make plausible suggestions, in relation to known neurological mechanisms of opioid pharmacology.

In the Introduction, I will review the scientific literature, summarizing some important effects of opioids, especially analgesia. From a historical perspective, I will describe what is currently known about opioid receptors and their distribution in the CNS, including the MGB. Then, I will discuss why I chose Mongolian gerbils as an animal model to study neurons of the auditory thalamus. For the reader's perusal, I will raise issues that are relevant to these investigations and the development of hypotheses for opioid actions.

1.1 Historical perspective

In humans, perceived pain is an unpleasant sensory and emotional condition, implied by the communication of the painful experience and overt body reactions to painful stimuli (Kandel et al. 2000). Some of the earliest ways of dealing with pain involved the ingestion of "opium" (a Greek word for juice), obtained from the poppy plant, *Papaver somniferum*. Substances from the poppy head have received use for pain relief for over a millennium (e.g., Egyptians during the reign of Cleopatra) although some claim that there is little evidence of opium use before the 11th century (Kirkup 1988). After isolation as an opium alkaloid in 1803, morphine has become and remains the standard treatment for relief from acute postoperative pain as well as for chronic cancer and neuropathic pain. Actions of morphine at its receptors or the inhibitory influence on other transmitter systems produce analgesia. Tolerance, dependence and, the withdrawal symptoms observed on abrupt discontinuation chronically treated with morphine in humans and experimental animals, are outstanding features of its pharmacology.

In the brain, morphine acts at membrane receptors on neurons characterized by a classical dose-response relationship or saturating function curve. For any drug, a demonstration of competitive antagonism would support the premise of drug-action at membrane receptors. The first report of a morphine antagonist was that of Pohl (1915) who studied N-allylnorcodeine. This substance inhibited the effects of morphine and produced a rightward, parallel shift in the dose-response relationship. In the 1940s, investigations of its cogeners led to the discovery of other morphine antagonists, including

nalorphine. Clinical investigation of nalorphine in the early 1950s revealed antagonism of morphine poisoning as well as the identification of unanticipated analgesic effects of nalorphine at higher doses. Whereas this represented the first instance of agonist/antagonist properties, nalorphine did not receive further clinical use because it caused anxiety and dysphoria. Following its synthesis, Blumberg et al. (1961) demonstrated that naloxone was a potent antagonist of morphine in experimental animals, at least ten times as active as nalorphine. Subsequent studies have shown that naloxone is a competitive antagonist of morphine with no analgesic or toxic properties of its own (Jasinski et al. 1967). Subsequently, naloxone has figured prominently in studies that have attempted to demonstrate the existence of morphine receptors.

In the 1960s, it was recognized that there were CNS mechanisms that can strikingly alter the perception of painful stimuli. A discovery that came from behavioural experiments on pain perception stimulated the rapid development of concepts about receptors for morphine and for substances endogenous to the brain. In 1969, Mayer completed a PhD thesis with startling observations that short-duration electrical stimulation of the periaqueductal gray of the mesencephalon resulted in a profound long-lasting analgesia in the rat. Subsequent studies from that laboratory revealed that naloxone also completely antagonized the analgesic effects of the electrical stimulation (Mayer et al. 1971). This ushered in a search for endogenous brain "opioids" or substances mimicking the effects of substances derived from the opium poppy. This culminated in the discovery of endogenous opioids (e.g., leu^5-enkephalin) in an unlikely tissue source, which were mouse vas deferens and guinea pig myenteric

plexus (Hughes et al. 1975) and stimulated the opiate-binding investigations of the early 1970s.

1.2 Opioid receptor-binding

In the early 1970s, the independent laboratories of Avram Goldstein, Eric Simon, Solomon Snyder and Lars Terenius demonstrated using tritiated opioid agonists, and later antagonists, opioid receptor-binding sites in the CNS of rodents (Goldstein et al. 1973; Pert and Snyder 1973; Simon et al. 1973; Terenius 1973). Throughout the neuraxis, these studies delineated stereospecific opioid receptor-binding mainly localized to areas primarily involved in the perception (e.g., limbic system in higher mammals) and reactive components (e.g., substantia gelatinosa of both trigeminal brainstem complex and spinal cord) of nociception.

The thalamus and periaqueductal gray area have pathways that are crucial for the transmission of nociceptive information to the cerebral cortex. The lateral thalamus controls somatotopic pain sensation, whereas the medial thalamus regulates pain influenced by emotions (Snyder 1977). In view of the limbic system functions associated with emotion and attention, the localization of opioid receptors to limbic areas implies that endogenous opioids mediate or modulate somatosensory inputs, including pain and emotional behavior. On the other hand, there are numerous reports that opioid antagonists like naloxone do not affect pain threshold measured under various conditions in humans (e.g., Gronroos and Pertovaara 1994; Olausson et al. 1986). In summary, the distribution of opioid receptor-binding is regional within the brain, to a certain

extent, depending on a functional involvement in the transmission, perception and emotional aspects of nociceptive processing. The actions of opioids at the receptor-sites on neurons can account for therapeutic and addictive effects of opioids (Kanjhan 1995).

1.3 Opioid receptors

Opioid receptors are classified into three major groups, μ, δ and κ receptors, based on differences in pharmacological actions (Pasternak 1993). In the older literature, there are descriptions of σ receptors as a fourth type of opioid receptor (Martin et al. 1976). SKF-10047, phencyclidine and cyclazocine are agonists that compete with each other at this receptor (Gilbert and Martin 1976a; Martin et al. 1976; Quirion et al. 1981). Since the three drugs have hallucinogenic properties, there is a hypothesis that drug actions at the σ receptor lead to dysphoric effects. Several clinically used opioids, including pentazocine, a partial agonist, and nalorphine which has almost disappeared from clinical use, stimulate the σ receptor (Gilbert and Martin 1976b; Martin et al. 1976). These and other opioids with agonist actions at the σ receptor, indeed, can produce clinically significant dysphoria (Gilbert and Martin 1976b). Naloxone does not antagonize some of the effects of σ agonists (Kemp et al. 1988). Hence, recent literature ignores σ receptors in the opioid receptor classification (Henderson et al. 1999). Studies using anti-sense technology and rat models have established the functional significance of these cloned receptors (Chen et al. 1993; Yasuda et al. 1993). Investigators have cloned members of each class

of opioid receptor from human cDNA and have obtained the respective amino acid sequences (Knapp et al. 1994; Wang et al. 1994; Zhu et al. 1995).

The three opioid receptor classes have subtypes, respectively identified μ_1 and μ_2, δ_1 and δ_2, and κ_1, κ_2 and κ_3 receptors (Pasternak 1993). Investigators have used agonists and/or antagonists to selectively label these receptor subtypes. Recently, an opioid receptor-like receptor (OP_4) has been cloned, joining the opioid receptor family (Bunzow et al. 1994). The effector mechanism for opioid receptors involves coupling via pertussis-sensitive GTP-binding proteins to inhibition of adenylyl cyclase activity (Childers 1991), activation of K^+-currents and depression of Ca^{2+}-currents (Duggan and North 1983).

All opioid subtypes have a role in reducing the intensity of pain (Pasternak 1993; Ho et al. 1997). Systemically administered morphine and many other opioids are more selective for μ_1 receptors than μ_2 receptors. The μ_1-effects are attributable to supraspinal interactions (Bodnar et al. 1988) whereas the μ_2-effects result from spinal interactions (Pick et al. 1992). Activation of μ_2 receptors produces analgesia and other prominent effects such as depression of respiration and gastrointestinal motility, pupillary constriction, euphoria, sedation and physical dependence (Fowler and Fraser 1994). While morphine action at μ_2 receptors there are suggestions that morphine actions at μ_2 receptors may produce dysphoria and psychomimetic effects, μ_2-receptor activation is associated with dependence (Reisine and Pasternak 1995).

Psychomimetic actions are not uncommon with pentazocine, a partial agonist at μ receptor, and are attributable to agonist interactions at κ_1 and κ_2 receptors. The analgesia produced by pentazocine is mostly attributable to

spinal interactions at κ_1 receptors (Reisine and Pasternak 1995). The absence of psychomimetic actions of pentazocine might reflect that a main site for this drug is spinal. Nalorphine may produce analgesia by activating κ_3 receptors (Paul et al. 1991).

Recent studies have implicated opioid actions at δ receptors in hormone regulation, feeding behaviour and peripheral analgesia. These receptors exist in supraspinal, hypothalamic-pituitary regions spinal, and peripherally in joints (Nagasaka et al. 1996). Whereas sufentanil is the only known clinical opioid with agonist actions at δ receptors (Freye et al. 1992), the peripheral analgesia recently demonstrated for morphine (reviewed by Herz 1996) may be partly attributable to its actions at δ receptors.

1.4 Practical rationale for animal studies

The distribution of opioid receptors in the CNS of gerbils, the animals used in the present investigations, is unknown, but is probably similar to the rat CNS. Using the extensively studied rat brain as a substitute, the MGB contains μ opioid receptors, but not κ- and δ-receptors or OP4 receptors according mRNA and immuno-histochemical studies (Ding et al. 1996; Mansour et al. 1994; Neal et al. 1999).

The role of opioid receptors is gradually being elucidated in the auditory system. As with neurons in other CNS areas, leu-enkephalin, an endogenous opioid peptide, may influence the development of the central auditory system (Kungel and Friauf 1995). Opioids have a role in increasing thresholds in several auditory tests in experimental animals. In chinchilla, intravenous administration

of (-)pentazocine, which has no affinity for σ receptors, increased the baseline values for the threshold of a compound action potential (Sahley and Nodar 1994). In comparisons of nociceptin receptor-knockout mice to wild-type mice, investigators have shown that thresholds for the auditory brainstem responses (ABR) became more positive in homozygote mice, without changing nociception or locomotion (Nishi et al. 1997). Opioids in the auditory system might have a role in perceiving pain stimulation. Lesions of the MGB block the hypoalgesia produced by white noise stress (Bellgowan and Helmstetter 1996). Systemic injection of naltrexone, a potent, non-selective opioid antagonist, has the same effect as lesioning the MGB (Helmstetter and Bellgowan 1994).

Generally speaking, the opioid system in thalamic nuclei, may regulate neuronal activity and also have a pathophysiological role, such as in generalized *absence* epilepsy. Recent studies have shown that the activation of opioid receptors in the thalamus may cause epilepsy in WAG/Rij rats, a genetic model for *absence* seizures (Przewłocka et al. 1998). The intrathalamic administration of D-Ala^2-N-methyl-Phe^4-Gly^5-ol-enkephalin (DAMGO), a μ-opioid receptor agonist, greatly increases the number of spike-wave discharges in the electroencephalogram (EEG). Given a thalamic origin for the epileptogenesis of absence seizures and the abilities of thalamocortical neurons to profoundly influence cortical activity (Steriade et al. 1997), such effects of DAMGO imply a pathophysiological role for opioids in the thalamus.

Among the thalamic nuclei, more specific sites have been studied with respect to the involvement of opioid receptors in the epilepsies. Intrathalamic injection of met-enkephlalin into the mediodorsal nucleus (Frenk et al. 1978), but

not a relatively μ-opioid receptor selective agonist, dermorphine, (Greco et al. 1994), induces epileptic discharges in rats. However, met-enkephalin microinjection into the centromedian nucleus of baboons does not elicit seizure activity behaviourally or in the EEG (Meldrum et al. 1981). The use of different strains of rats or other species might account for the differing effects of μ receptor activation. Systemic and intracerebroventricular injections of numerous opioid agonists induce different effects of opioids in various animal species (Meldrum et al. 1981). Furthermore, met-enkephalin is a mixed agoinst at μ and δ opioid receptors and both μ and δ opioid receptors exist in the mediodorsal nucleus (Mansour et al, 1995). Hence, the different observations might be due to diverse functions of μ and δ opioid receptors.

If the activation of opioid receptors in the thalamus has excitatory effects on neurons, the number of receptors would be small if they maintain inhibitory neuronal activities. Conversely, autoradiographic studies have demonstrated that opioid receptor binding in several brain sites of seizure-sensitive gerbils during pre-seizure states was larger than the opioid receptor binding of seizure-resistant gerbils (Lee et al. 1986). MGB was one of the sites that had significantly higher opioid binding activities. The epileptic events diminished the opioid receptor binding in seizure-sensitive gerbils. Therefore, the activation of endogenous opioid receptors may have an anti-convulsant effect.

Frey and Voits (1991) suggested that opioids have a pathophysiological role in *absence* seizures. They deduced this from the observations that systemic administration of opioids increase spike-wave discharge and endogenous opioids suppress tonic-clonic seizures. However, their hypothesis does not explain the

observations that injection of opioids into certain area of the thalamus did not induce seizures. Most plausible explanations may invoke the thalamic activation of opioids having dual effects on seizures.

1.5 Questions asked in these investigations

Typically, opioid actions on neurons are inhibitory, however opioids also might have excitatory effects. Electrophysiological studies have shown their inhibitory effects on various cells, e.g., locus coeruleus neurons (North and Williams 1985) and the centrolateral thalamic neurons (Bruton and Charpak 1998). Thus far, three groups have studied the effects of opioids on the auditory system (Chan-Palay et al. 1982; Lin and Carpenter 1994; Sulaiman and Dutia 1998; Sulaiman et al. 1999). In the vestibular nucleus, Chan-Palay et al. (1982) and Sulaiman and Dutia (1998) have demonstrated the inhibitory effects of opioids, i.e., an increased membrane conductance, hyperpolarization and reduction of firing rate. On the other hand, Lin and Carpenter (1994) have shown that morphine increase firing frequency.

Using morphine or DAMGO applications, I studied the effects of opioids on neurons of the gerbil MGB and asked the following questions:

(1) What effects do opioids have on membrane properties of MGB neurons?

(2) If opioids have inhibitory or excitatory effects on MGB, which membrane currents or channels are involved?

2. Methods

2.1 Preparation of slices

The animal experiments were conducted according to the guidelines approved by the Committee on Animal Care of the University of British Columbia and in compliance with guidelines of the Canadian Council on Animal Care.

2.1.1 Surgical preparation. For each experiment, I used two Mongolian gerbils, *Meriones unguiculatus*, of either gender (9-16 days). They were deeply anesthetized with halothane (MTC Pharmaceuticals, Ontario, Canada). Each gerbil was placed into a wide-mouth, 350 ml bottle containing two cotton balls saturated with ~1.8 ml of halothane. As an approximate endpoint for deep anesthesia, I observed the respiratory movements at the level of the gerbil's abdomen; just before respiration ceased completely, the gerbil was taken out of the bottle. The animal was decapitated by with a scalpel. A midline incision was made in the dorsal dermis of the head. The midbrain was severed with a stainless steel spatula at ~0.1 cm away from the decapitated site, facilitating reflection of the brain from the cranium vault. The brain was rapidly removed from a cranial cavity by a stainless steel spatula. The brain was immersed in ice cold (1-4 °C) artificial cerebrospinal fluid (ACSF) containing sucrose as a replacement for NaCl for 5-7 min in a 20 ml beaker. The glass container was placed on ice. The entire surgical procedure required less than 1.5 min.

2.1.2 Physiological solutions. Normal ACSF was used for most of the experiment and a modified ACSF was used for the slice preparation. The "normal ACSF" contained (in mM): 124 NaOH, 26 $NaHCO_3$, 10 dextrose, 2.5 KCl, 2 $CaCl_2$, 2 $MgCl_2$, and 1.25 KH_2PO_4. For the preparation of slices, a "modified ACSF" contained a low [Na^+], substituted with approximately equimolar sucrose (125 mM). The low [Na^+] ACSF was used to enhance the viability of the slices (Aghajanian and Rasmussen 1989). For use, the solutions were saturated with 95% O_2/5% CO_2. The pH of a saturated solution was 7.4, measured by a pH meter (pH Meter 215, Corning, NY or 30Φ pH meter, Altex-Beckman, USA).

2.1.3 Tissue slicing. On the morning of an experiment, a 250 ml beaker of modified ASCF, previously saturated with 95% O_2/5% CO_2, was kept in a freezer for 90 min until an ice-slurry formed. After removal from the cranial vault, the brain was cut into a block that measured 0.8 cm x 0.8 cm, containing the medial geniculate nuclei of both hemispheres, and placed on a filter paper soaked with modified ACSF, bubbled with 95% O_2/5% CO_2, in a Petri dish. I cut the brain in two along the midline with a double-edge razor blade (Personna, VA, USA). The blades were cleaned with methanol-soaked tissue paper to remove the manufacturer's oil. The blades were snapped in half at the middle such that one edge could be used for cutting the brain and the other for making slices. The first cut was parallel to, and ~0.5 cm away from the decapitation plane. Then, the brain was trimmed to a block by making two cuts, each parallel to, at ~0.4 cm from the midline, in the lateral aspects of the cerebral hemispheres. After this trimming, the block was returned to the Petri dish for a few

minutes until the plastic stage was prepared with α-cryanoacrylate glue (Acuu-flo 8 or Instantbond 8, Lepage, Ontario, Canada). The plastic stage was set in the bath of a Vibratome slicer (Campden Instruments, London, England), filled with the ice-slurry of modified ACSF. A small amount of the glue was spread on the stage with the tip of the glue container. The block was removed from the Petri dish with a stainless steel spoon-shaped spatula. Excess ACSF around the tissue-block on the spatula was removed as much as possible with the capillary action of filtered paper. The block then was placed onto the stage, inserted into the Vibratome, and modified ACSF was poured into the bath, covering the block by ~1 mm. Coronal sections of the brain were cut at 300 μm. The cutting speed of the Vibratome was adjusted such that white matter was cut more slowly than the grey matter of the brain.

2.1.4 Incubation of slices. After cutting, the slices were gently lifted and placed into a 250 ml beaker containing normal ACSF. The beaker had a fine plastic mesh screen and the slices descended onto this screen which was ~0.5 cm below the level of normal ACSF. They were allowed to warm up gradually to 30-33 °C. Slices were incubated for 1 hour in normal ACSF (pH 7.4), saturated with 95% O_2/5% CO_2 and maintained with gentle bubbling so as to avoid agitation.

After the initial heating, they were allowed to return to room temperature (23-25 °C). I used these slices for up to 3 hours after the incubation.

2.2 Electrical recording

Slices containing the medial geniculate nuclei, were identified visually by a dissection microscope. The medial geniculate nuclei were identified as protruded sections from the brain. The slices were transferred using a glass tube to the recording chamber of the microscope. There, the slices were stabilized on a nylon mesh with a platinum wire ring. The slices in the recording chamber, (volume ~1 ml) made from Plexiglass, were superfused by gravity with aerated normal ACSF at a flow rate of ~1.5 ml/min continuously bubbled with 95% O_2/5% CO_2.

2.2.1 Microelectrodes. The electrodes were made from borosolicate glass tubing with filaments (WP, Instruments, Sarasota, Florida, USA) and drawn with a puller (Narishige Instruments, Japan). Adjustment of the puller settings allowed me to obtain electrode resistances of 5 to 9 MΩ. The electrode solution contained (in mM) 140 KOH, 5 KCl, 10 ethylene-glycol-*bis*-(β-aminoethyl ether)- *N,N,N',N'*-tetraacetic acid (EGTA), 4 NaCl, 3 $MgCl_2$, 10 *N*-[2-hydroxyethyl] piperazine-*N'*-[2-ethane-sulfonic acid] (HEPES; free acid), 1 $CaCl_2$, 2.8-3 Na_2·ATP or Mg·ATP, and 0.3 Na·GTP. Just before the experiment, 2.8 to 3 mM Na_2·ATP or 3 Mg·ATP, and 0.3mM Na·GTP were added to this solution. The electrode solution was adjusted to pH 7.4 with 50 % gluconic acid. A 30 gauge synthetic needle connected to a 1 ml syringe was used to fill an electrode with the solution.

2.2.2 Electrical hardware. Current-clamp whole-cell patch clamp recordings from MGB neurons were performed with an Axoclamp 2B amplifier (Axon Instruments,

Foster City, CA). The recordings were made at room temperature (23-25 °C). Signals were lowpass filtered at 5 kHz, digitized at 10 kHz with a 12 bit data acquisition board (TL1, Scientific Solutions) in a Pentium computer, using pClamp 6 software (Axon Instruments, Foster City, California). Data acquisition, storage and analysis were done by pClamp 6.0.4 software running on a Pentium computer.

2.2.3 Microelectrode advancement. I visually observed the cells in the slice with differential interference contrast microscopy (Zeiss Axioscope FS) with white or infrared illumination. The images were displayed on a video screen (Sony, Japan). The cells were selected visually for microelectrode recording. Before approaching a cell with an electrode, I visually confirmed that there was no contamination at the electrode tip, applying a gentle positive pressure (~100 millibars) to the syringe. This pressure was maintained and controlled manually with a 10 ml syringe, connected to the electrode and holder assembly (Axon Instruments) by plastic tubing. Approaching the cell with an electrode was accomplished in micrometer advancements under manual and visually aided control using a micromanipulator (Narishige Instruments, Japan). On mechanical communication of the electrode tip with the cell, the postive pressure was reduced to zero. A gigaohm seal was established between the electrode and the cell by suction with the 10 ml syringe. Additional suction was applied with the lips to break through the cell membrane, achieving the whole-cell configuration (Edwards et al. 1989).

2.2.4 Electrical parameters. I distinguished neurons from glial cells by evoking action potentials with depolarizing current pulse injections. The resting membrane potentials were usually ~–60 mV in most neurons, after correction for tip potential. The conductance of the each neuron was calculated using Ohm's Law ($G = \Delta I / \Delta V$) from the steady-state voltage response to hyperpolarizing current pulses (1000 ms duration) of less than 10 mV amplitude injected into a neuron. The conductance also was obtained from the main linear portion of the slope in the current-voltage relationships derived from a composite of such responses.

2.2.5 Recording stability. Generally, the recording conditions (resting membrane potential, input resistance) were stable, commonly for hours. This was verified by visual observations of the pipette-neuron "patch" condition. When it was apparent that the communication between the electrode and the neuron was compromised, e.g., by debris, plugging of the tip, distortion of the neuron due to the electrode), the recording was abandoned. All voltage values were later corrected for a liquid junction potential of –11 mV (Tennigkeit et al. 1997).

2.3 Pharmacological agents

Stock solutions of the drugs used in these experiments were prepared using distilled water or normal ACSF and frozen until needed. Morphine hydrochloride was obtained from F.E.Cornell & Co. Ltd. (Montreal, Canada). Naloxone was purchased from Sigma Chemical (Canada) and Endo Laboratories (New York, USA). [D-Ala^2,N-Me-Phe^4,Gly-ol^5]-enkephalin (DAMGO), N-methyl-D-glucamine

(NMDG), $BaCl_2$ and tetrodotoxin (TTX) were purchased from Sigma Chemical (Canada). Stock solutions were freshly diluted with normal ACSF before each experiment. The drug solutions were kept in inverted 60 ml plastic syringes and bubbled with 95% O_2/5% CO_2. The five syringes were connected to the recording chamber with polyethylene tubing for purposes of applying ACSF or drugs by gravity flow. The outflow of each syringe was controlled manually with a valve to change the type of application. The volumes within the reservoirs were adjusted such that a change from solution to another occurred with minimal flow disruption due to differences in hydrostatic pressure. When I only changed syringes without applying morphine, I call it "sham applications" and showed "0 μM" in the present thesis. Drug(s) were applied for a duration (3 min) that would allow a reasonable assumption that steady-state concentrations had been achieved in the bath and tissue. Both control and drug applications were at a rate of 1.5 ml/min. It took at least 1.5 min for the 'leading edge' of a solution to reach the recording chamber.

2.4 Data and statistical analyses

The data are presented as means ± S.E.M. and represent observations made in different, visually identified neurons of slices that had been exposed to drugs. In most cases, once an experimental protocol involving morphine application was complete, the slice was discarded and replaced with a fresh slice before further experimentation. Representative graphs were constructed using Corel Draw version 8.0 software (Corel, Ottawa, Canada) or Prism version 2.0 software (Graphpad, San Diego, U.S.A.). The data were analysed by Clampfit of pCLAMP 6.0.4. or Prism

version 2.0 software. Different conditions of experiments were assessed with a Student's unpaired t-test (two-tailed p value). A Bonferroni post test was used to compare means of different concentration applications. I used one sample t-test to analyse in the same condition to evaluate the difference from estimated population means. The data were considered significant if there were less than a 0.05 chance that they would occur randomly ($P<0.05$). EC_{50} of concentration-response curve was estimated by sigmoidal concentration-response curve fits by Prism version 2.0 software. The latter spike half-width was measured the spike-half width after the peak of action potentials.

3. Results

I analyzed the results from neurons with resting potentials that were –50 mV or less (corrected for junction potentials). The action potentials evoked with current pulse injection generally had amplitudes of ~60 mV (cf. Fig. 3.1). If the input resistance (R_i) was extremely high, I considered the possibility of electrode tip plugging by debris. With the aid of DIC-microscopy, I often visually confirmed this situation and usually terminated the experiment. In any case, I chose neurons with a R_i of <1000 MΩ for analysis.

Control data were selected according to the following: "Group 1" where applications of morphine started >8 min after establishing a whole-cell configuration; and, "Group 2" where morphine applications were made ~3 min after formation of the electrode-neuron seal.

3.1 Passive membrane properties

The average resting membrane potential (V_r) was –59.2 ± 1.1 mV (n = 21) in Group 1 and –58.5 ± 1.5 mV (n = 11) in Group 2. The input conductance (G_i) or $1/R_i$, (see Methods) ranged from 1.01 to 6.02 nS (R_i = 989 to 166 MΩ). The average G_i in Group 1 was 2.4 ± 0.2 nS (R_i = 501 ± 46 MΩ; n = 21) and in Group 2, 1.9 ± 0.2 nS (R_i = 601 ± 59 MΩ; n = 11). The mean membrane time constant (τ_m) was estimated from single exponential fits. For this analysis, I used only data from neurons that were well-fitted by a single exponential curve. The average τ_m was in Group 1, 56 ± 4.3 ms (n = 17) and in Group 2, 75 ± 9.1 ms (n = 10). Using an unpaired t-test, means of the V_r and the G_i between Group 1 and Group 2 were not

significantly different ($p = 0.6756$ for the V_r; $p = 0.1909$ for the G_i), but not means of the τ_m ($p = 0.0432$).

3.2 Firing modes

Strictly speaking, it often was difficult to evoke only a single action potential on current injection. Therefore, I have defined "just-threshold" for action potential firing (V_{thr}), as the voltage value resulting from a minimal amount of injected current required to evoke one or more action potentials for about 50% of consecutive recordings in a neuron.

The V_{thr} was in Group 1, -50.1 ± 1.5 mV (n = 21) and in Group 2, -40.8 ± 1.6 mV (n = 11). When I observed >1 spike, even by the minimum current for the just-threshold criterion, I used the first spike for the analysis of spike amplitude and half-width. The mean spike amplitude was in Group 1, -61.6 ± 2.5 mV (n = 21) and in Group 2, 59.7 ± 2.3 mV (n = 11). The mean spike half-width was in Group 1, 2.52 ± 0.15 ms (n = 21) and in Group 2, 2.95 ± 0.23 ms (n = 11). By an unpaired t-test, means of the V_{thr} between Group 1 and Group 2 were significantly different ($p = 0.0005$). On the other hand, means of spike amplitude and spike half-width between Group 1 and Group 2 were not significantly different ($p = 0.6233$ for spike amplitude; $p = 0.1190$ for spike half-width).

With current pulse injection, the neurons exhibited tonic firing on depolarization from the resting potential or from threshold (Fig. 3.1.A). When the neurons were hyperpolarized by DC-current to <–80 mV, depolarizing current-pulse injection led a single spike or spike bursts that included a low threshold Ca^{2+} spike

(LTS; Fig. 3.1.B). I used neurons from relatively young MGB gerbils, however, I did not observe the spike doublets on depolarizing current injection as in previous studies of young rat neurons in the ventral partition of the MGB (Tennigkeit et al. 1998). I sometimes could not detect an LTS on the depolarizing responses, or rebound LTS following hyperpolarizing current pulse injection, in neurons near the resting potential. The lack of an LTS feature can imply that the neurons are interneurons (Pape and McCormick 1995; Pape et al. 1994). Or, since immature rat neurons do not apparently have an LTS (Tennigkeit et al. 1998), the absence of an LTS may reflect a development stage related to the age of gerbil.

Thus far, there are no studies in the literature, examining the ratio of interneurons to thalamocortical neurons in the gerbil MGB. Winer et al. (1988) reported that in Sprague-Dawley rats, immunoreactive neurons, expressing glutamic acid decarboxylase (GAD) or γ-aminobutyric acid totaled only ~1 % (Winer and Larue 1988). Gerbil brain has a distribution of GAD-positive neurons that is analogous to that of the rat, where the activity of GAD in the whole brain or thalamus is higher than in gerbils (Chalmers et al. 1970). In view of the above and absence of more information, I considered neurons with no LTS as thalamocortical neurons, and included them in my analysis.

I will first deal with the effects of morphine in sub-threshold membrane properties and then, return later to the effects of morphine in action potentials.

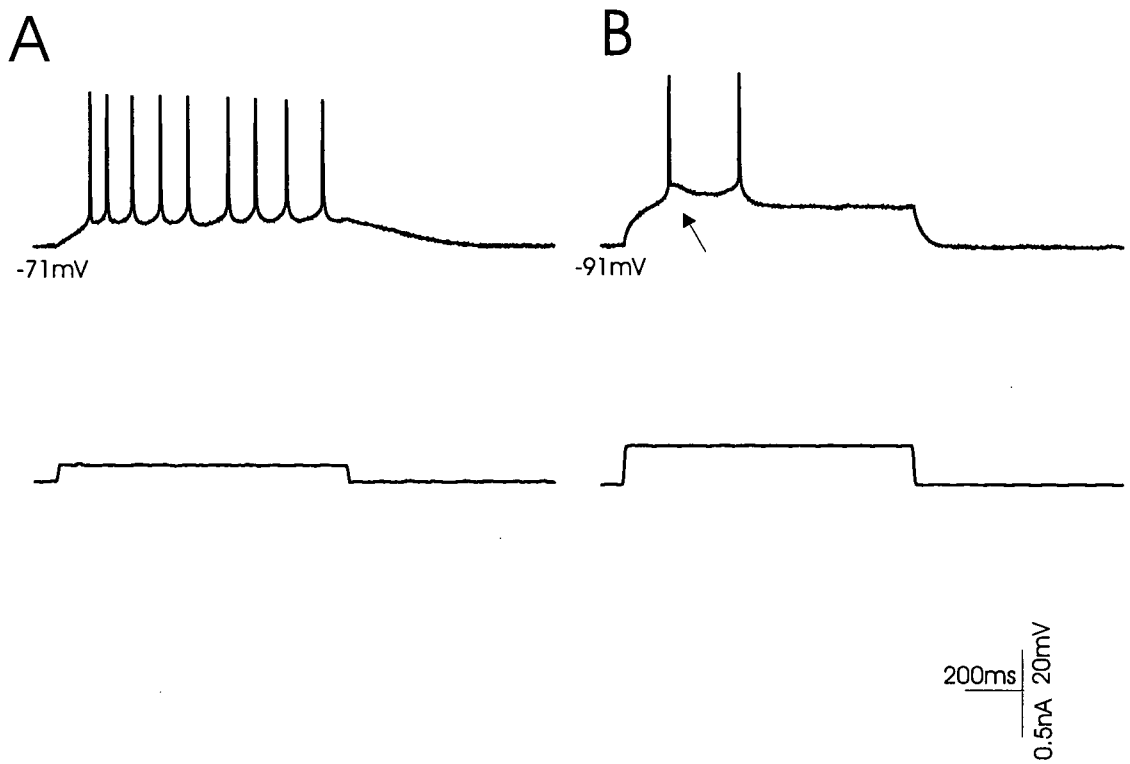

Fig. 3.1. Firing modes of gerbil MGB neurons.
The cell produced a tonic firing mode, held at –71 mV (A) and a burst firing mode, held at –91 mV (B). Arrow indicates a low threshold Ca^{2+} spike (LTS). For the rest of the figures in the present experiments, on the scale, the upper line indicates voltage and the lower line indicates current.

3.3 Effects of morphine on membrane properties

Application of morphine produced both increases (Fig. 3.2) and decreases (Fig. 3.3) in input conductance (G_i). Figure 3.4 and Table 3.1 show data from Group 1 and Figure 3.5 shows data from Group 2. I only used two different concentrations for Group 2. The effects were irreversible (Fig. 3.2), despite washing for periods longer than 30 min. I did not observe a reversal of the induced conductance change in either direction, despite long washout periods (e.g., 1 to 2 hrs). As shown in Figure 3.2 and extensively below, applications of naloxone, a non-specific opioid antagonist, also did not seem to accelerate the recovery from morphine application, i.e., reverse morphine's effects, even when naloxone was applied after a washout period of longer than 20 min. The change in the G_i did not apparently depend on the initial value of G_i, at all morphine concentrations (Fig. 3.6). Compared to Figure 3.4, eight out of eleven neurons in Figure 3.5 exhibited a remarkable increase in G_i on morphine application. The extent of the increased G_i had an impact on the difference in the concentration-G_i response curves between Groups 1 and 2 (Figs. 3.4.A and 3.5). The largest response was an 80.33 ± 45.41% increase, normalized to the initial G_i in the 10^{-8} M morphine group. The increase in G_i at the same concentration from Group 1 was 7.24 ± 5.33 %. In Group 1, the higher concentrations of morphine produced greater increases in G_i in a larger number of neurons.

Figure 3.4.B shows the G_i responses, calculated in the same way as above, to injected depolarizing current pulses. The concentration-dependent G_i responses to morphine were quite similar to those obtained with hyperpolarizing pulses. On the

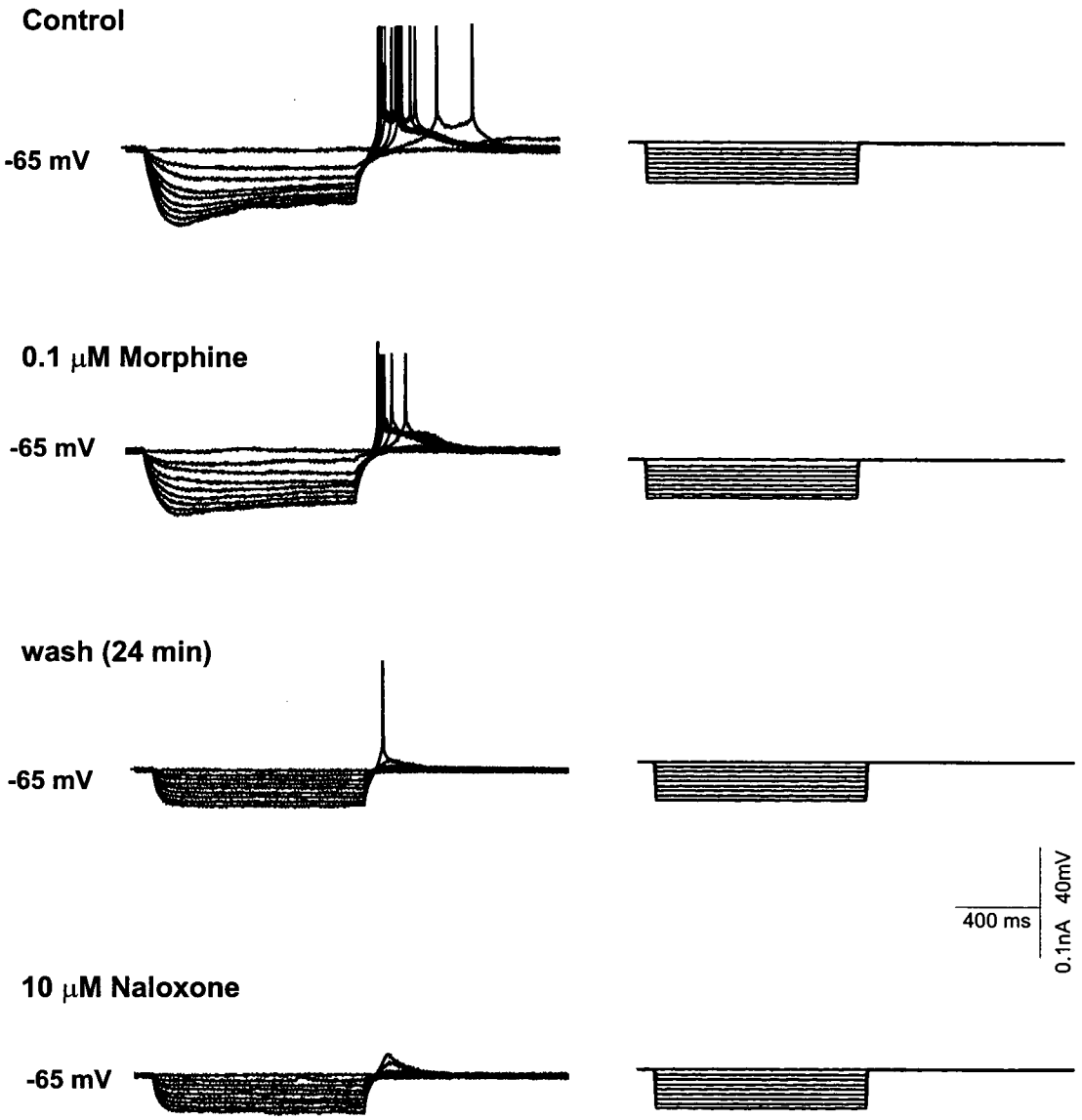

Fig. 3.2. Effects of morphine on input conductance (G_i).
An application of morphine (0.1 μM) for 3 min increased the input conductance by 126 %. The application of morphine started ~3 min after establishing a whole-cell configuration. The increased G_i produced by morphine was not reversible by washing for > 30 min and or by subsequent application of naloxone (10 μM for 3 min) and observation for an additional 5 min.

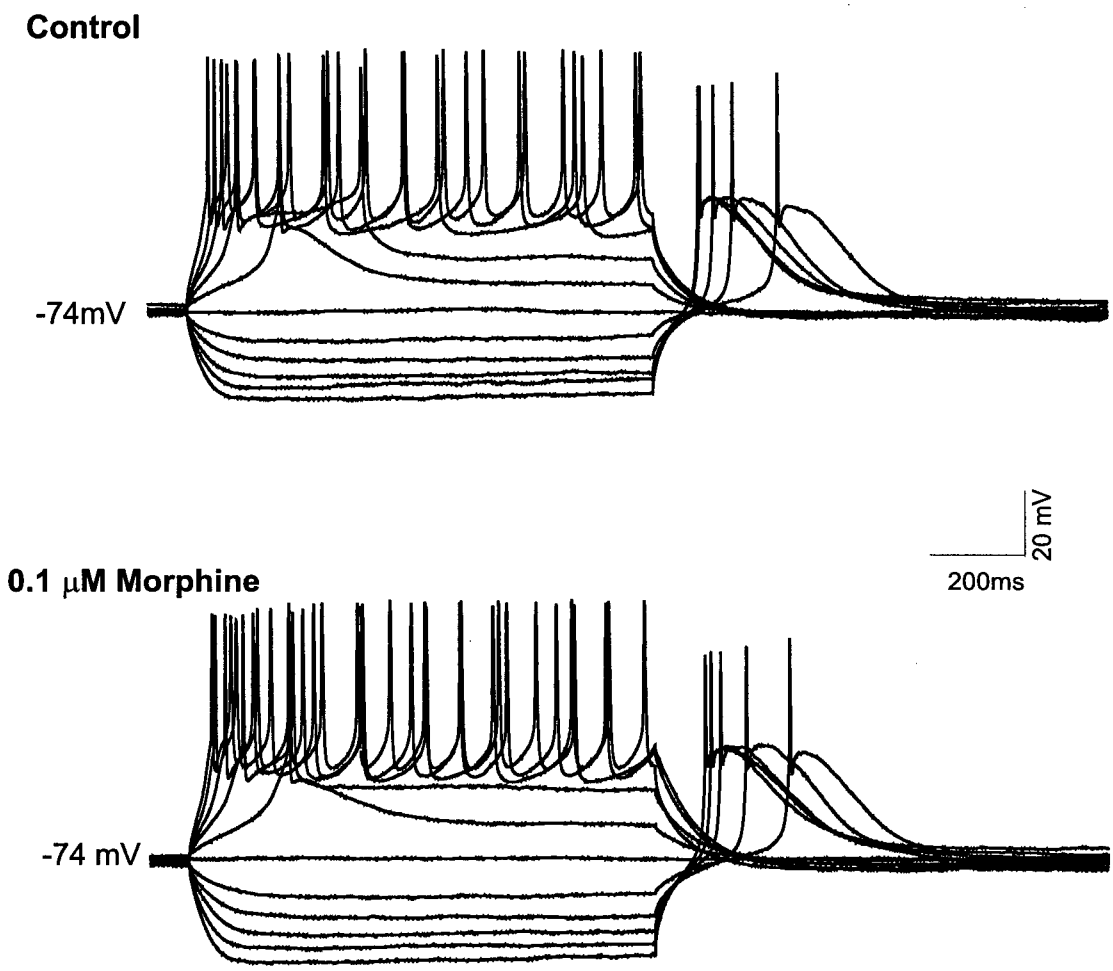

Fig. 3.3. Morphine decreased input conductance.
Application of morphine for 3 min (0.1 μM) decreased the initial input conductance by 36%. The responses were obtained during a cumulative application of morphine (0.1 nM to 0.1 μM). The current-voltage relationship was shown in Fig. 3.10.

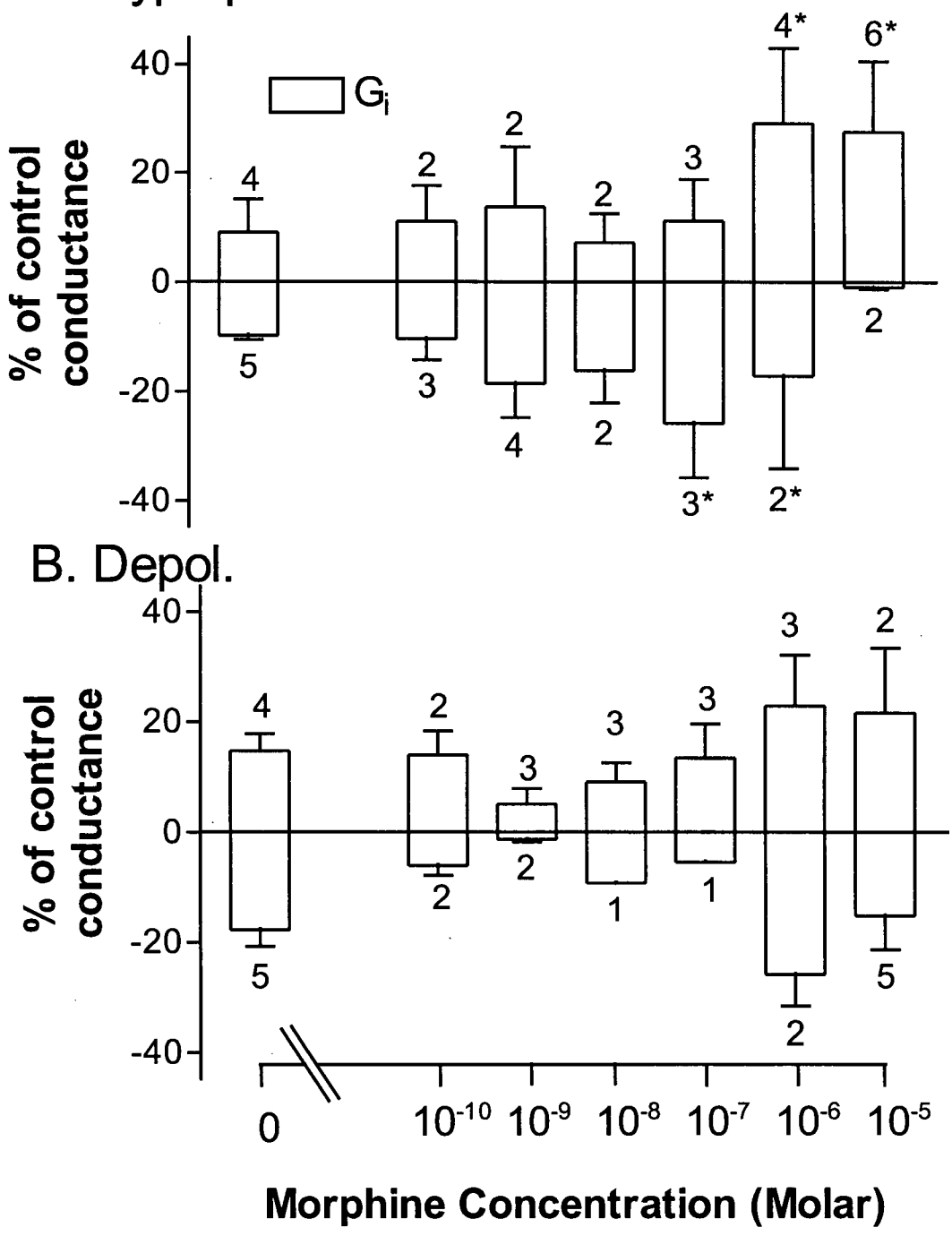
A. Hyperpol.
B. Depol.
% of control conductance
G_i
40
20
0
-20
-40
4
5
2
3
2
4
2
2
3
3*
4*
2*
6*
2
4
5
2
2
3
2
3
1
3
1
3
2
2
5
0
10^{-10}
10^{-9}
10^{-8}
10^{-7}
10^{-6}
10^{-5}
Morphine Concentration (Molar)

Fig. 3.4. Effects of morphine on input conductance (G_i). (previous page) For each neuron, the change in G_i was normalized to the initial input G_i. Application of morphine began > 8 min after establishing a whole-cell configuration. Morphine concentration is 0 μM stands for sham applications. Number of neurons at each concentration is indicated above and below the bars. A: Responses to injected hyperpolarizing current pulses (1000 ms duration). Using a Bonferroni post test, we analyzed the population mean difference in G_i relative to the G_i change in asterisk-marked neurons. In the increased G_i, there was no statistically significant difference between the 10^{-7} M group or the 10^{-8} M group or sham applications. In the decreased G_i group, the changes in G_i in the asterisk-marked neurons are not statistically different from neurons at the 10^{-8} M group or the 10^{-10} M group or sham applications. B: Responses to injected depolarizing current pulses (1000 ms duration). The G_i was calculated as we described in the Methods. The steady-state voltage response was obtained without the presence of action potentials. We injected depolarizing current pulses at ~10-20 pA into the neuron. Data from three out of 38 neurons include neurons with ΔV_r responses that were 10 to 11.5 mV in amplitude. The concentration-response curve of the increased G_i was similar to that of Fig. 3.3.A, but not of the decreased G_i. The number of neurons in the decreased G_i increased at the higher concentration of morphine.

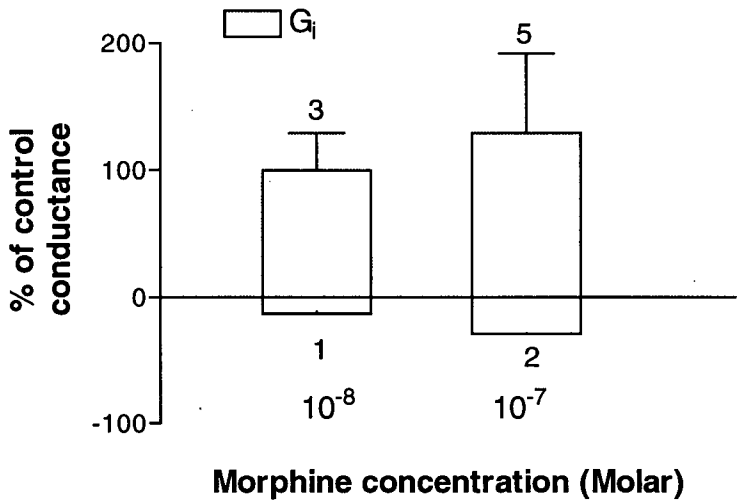

Fig. 3.5. Effects of morphine on input conductance (G_i).
For each neuron, the change in G_i was normalized to the initial input G_i. The application of morphine began ~3 min after establishing a whole-cell configuration. Note the different percentage scale from Fig. 3.4.

Table 3.1. Effects of morphine on input conductance (G_i)

Increased G_i

Morphine Concentration (Molar)	G_i (% of control)	P value	n
0	9.11 ± 6.00	0.23	4†
10^{-10}	11.11 ± 6.51	0.34	2
10^{-9}	13.75 ± 11.05	0.058	2
10^{-8}	7.24 ± 5.33	0.40	2
10^{-7}	11.21 ± 7.56	0.28	3
10^{-6}	29.32 ± 13.57	0.12	4
10^{-5}	26.72 ± 13.04	0.088	6

Decreased G_i

Morphine Concentration (Molar)	G_i (% of control)	P value	n
0	9.8 ± 0.71	0.0002	5†
10^{-10}	10.40 ± 3.80	0.11	3
10^{-9}	18.55 ± 6.19	0.019	4
10^{-8}	16.17 ± 5.89	0.11	3
10^{-7}	25.74 ± 10.01	0.24	2
10^{-6}	17.16 ± 16.86	0.49	2
10^{-5}	0.84 ± 0.41	0.29	2

† Since we used five syringes, the data were obtained from three different neurons by sham applications.

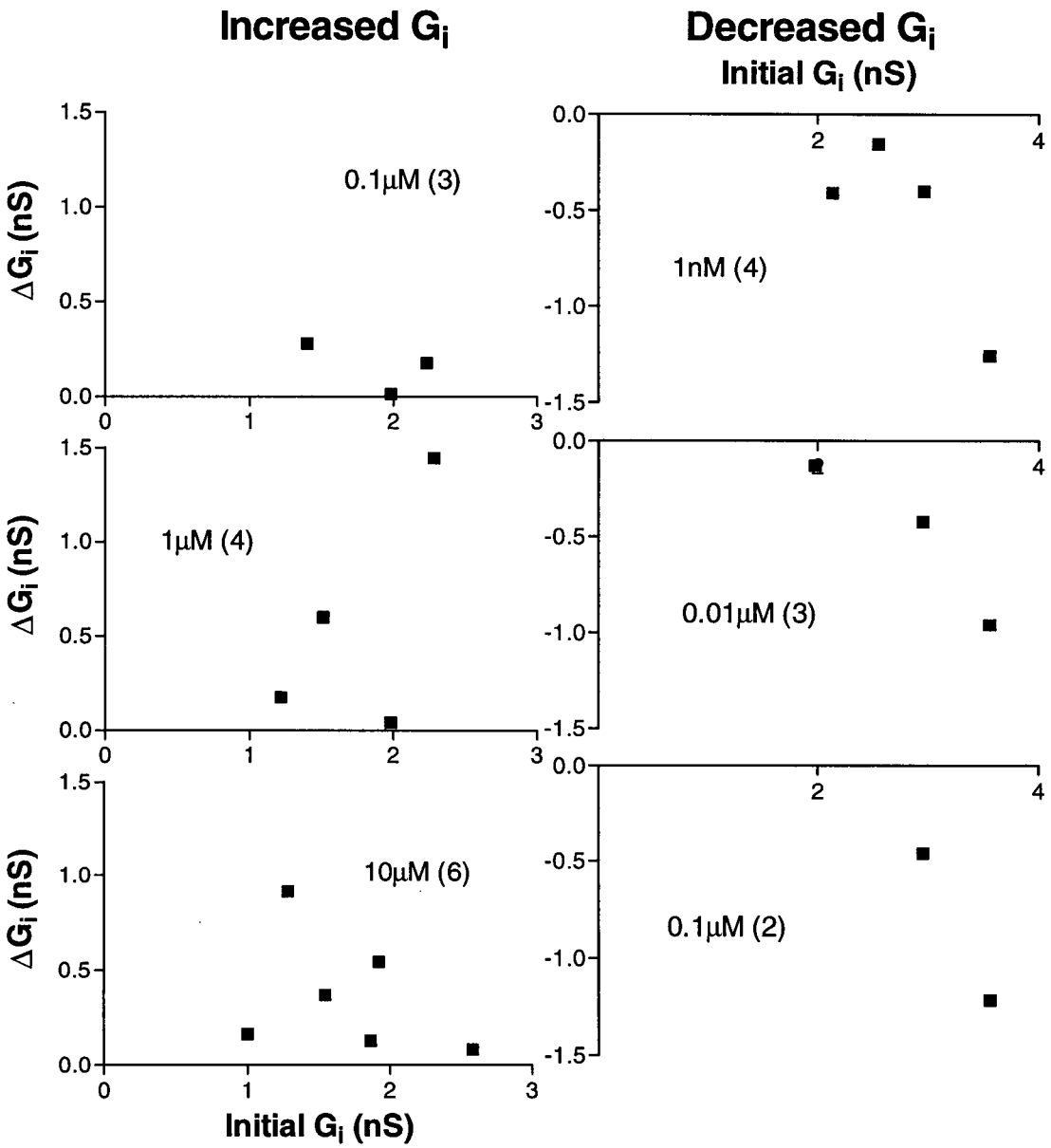

Fig. 3.6. Relationship of the changes in input conductance (G_i) to initial input conductance (G_i).
The application of morphine in 5 different concentrations changed G_i to hyperpolarizing current pulses. The changes tended to be independent of the initial G_i at all concentrations. We chose data at the concentration where there were significant effects on conductance (see Fig. 3.4.A). The number of neurons is indicated in parentheses.

other hand, in the decreased G_i category, the two sets of responses showed dissimilar trends. At concentrations of morphine less than 10^{-6} M, a decreased G_i was observed in fewer neurons tested with depolarizing pulses than with hyperpolarizing pulses. An extensive comparison would require a greater number of experiments at low morphine concentrations, particularly with depolarizing test pulses. At the higher concentrations of morphine, different from the response to hyperpolarizing current pulses, most neurons decreased the G_i with depolarizing current pulses.

In Figure 3.4.A, I compared the asterisk-marked increases in G_i and increases in G_i evoked by 10^{-8} and 10^{-7} M concentrations of morphine and sham applications. I also compared the asterisk-marked decreases in G_i and the decreases in G_i evoked by 10^{-10} and 10^{-8} M concentrations of morphine and sham applications. Whereas one might assume sigmoidal concentration-response relationships in Fig. 3.4.A for the mean changes in G_i in neurons tested with hyperpolarizing pulses, a Bonferroni post test showed that the population mean difference was not statistically significant with regard to asterisk-marked bars. Using sigmoidal concentration-response curve fits (see Methods), an estimate of the EC_{50} in the increased G_i category (hyperpolarizing test pulses) was 3.18×10^{-7} M. An estimate of the EC_{50} in the decreased G_i category (hyperpolarizing pulses), consisting of responses to 10^{-10} M and 10^{-7} M, was 8.91×10^{-8} M.

Morphine application typically hyperpolarized the membrane potential (V_r; Figs. 3.7A and 3.7B). In neurons where morphine increased G_i, the V_r hyperpolarized by 1-5 mV. The frequency of hyperpolarizations increased at

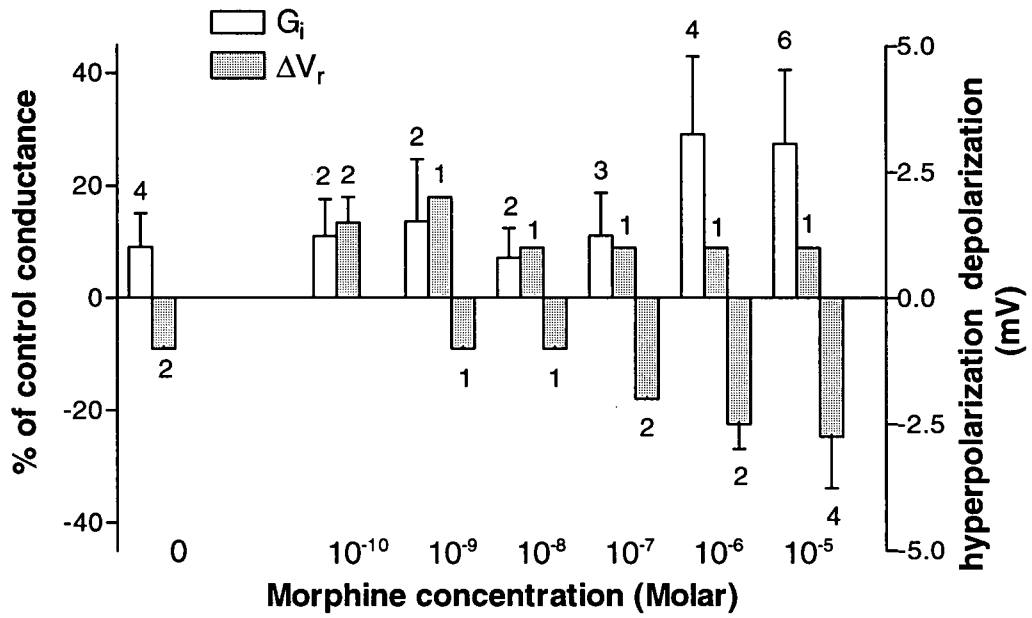

Fig. 3.7A. Relationship of morphine-induced increase in input conductance (G_i) to membrane potential (V_r).
The V_r was recorded at 3 min after starting application of morphine. The V_r hyperpolarized at higher concentrations of morphine. One cell at 10^{-5} M and 10^{-6} M, and two cells by sham applications did not change the V_r.

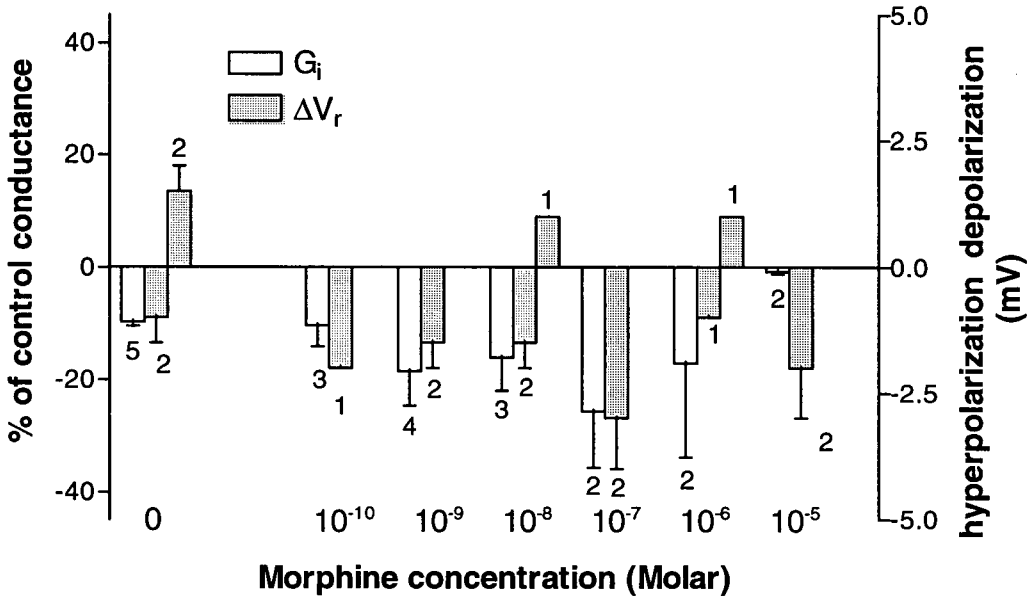

Fig. 3.7B. Relationship of morphine-induced decrease in input conductance (G_i) to membrane potential (V_r).
The V_r was recorded as for Fig. 3.7A. Application of morphine hyperpolarized V_r in most neurons. One cell by sham applications, and two cells at 10^{-9} M and 10^{-10} M, morphine did not change the V_r.

higher concentrations of morphine. In the case of decreased G_i (Fig. 3.7B), morphine hyperpolarized V_r in most neurons. In summary, I observed a hyperpolarization in response to morphine application, despite the direction of the induced G_i change.

The morphine-induced change in membrane time constant (τ_m) was almost correlated to the change in G_i, when G_i was increased (Figs. 3.8A), but not when G_i was decreased (Fig. 3.8B). As described above, I estimated the τ_m from the fit with a single-exponential curve. I excluded neurons that did not apparently fit the curve, i.e., when the fit was not exact, τ_m was very large. The bias might cause the large increase in τ_m observed with 10^{-5} M morphine (Fig. 3.8.A). Alternatively, morphine could affect the input capacitance especially at the higher concentration. When morphine decreased G_i, there was no association between the change in G_i and τ_m.

The reversal potential for morphine was determined from the intersection of control and morphine curves in the current-voltage relationship (Fig. 3.9). The mean reversal potential in the increased G_i, was -61.3 ± 6.4 mV (n = 3) in Group 1 and –68.2 ± 2.3 mV (n= 9) in Group 2. The calculated K^+-equilibrium potential is -85 mV, which implies that morphine activates several ion channels as well as K^+ channels. In neurons with a morphine-decrease in G_i, the current-voltage relationship demonstrates that the decrease of the slope conductance caused by morphine was clear when the V_r was > -80 mV (Fig. 3.10).

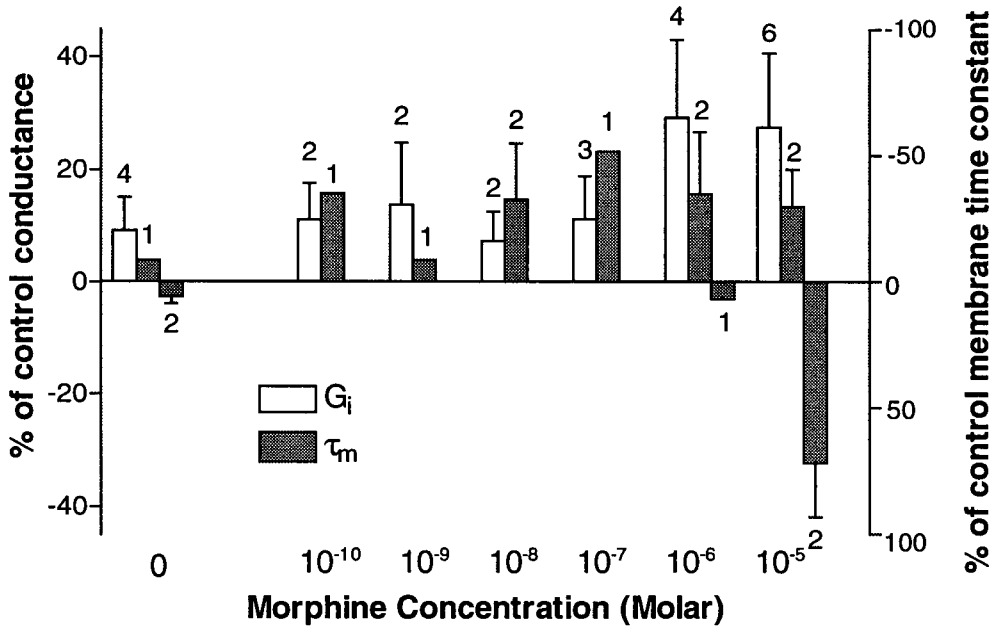

Fig. 3.8A. Relationship of morphine-induced increase in input conductance (G_i) to membrane time constant (τ_m).
The τ_m was estimated using a single exponential fit. When the trace did not apparently fit a single exponential curve, we omitted the cells from this figure.

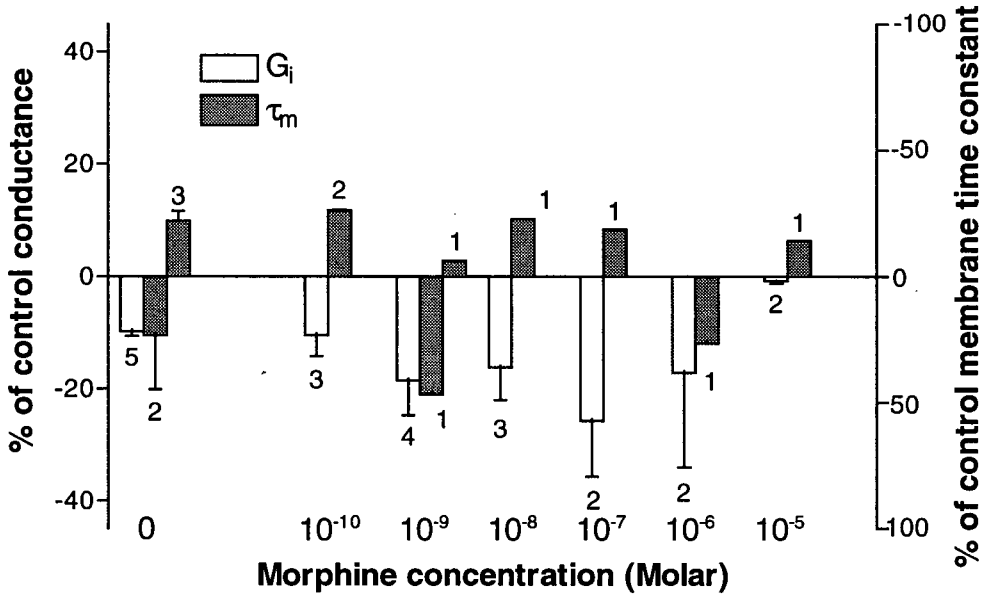

Fig. 3.8B. Relationship of morphine-induced decrease in input conductance (G_i) to membrane time constant (τ_m).
The τ_m was analyzed and chosen in the same way as in Fig. 3.8A. The τ_m decreased in most neurons and was not correlated to the change in G_i.

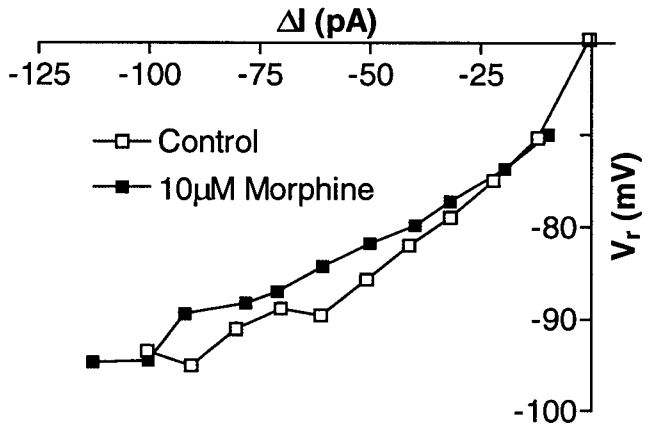

Fig. 3.9. Current-voltage relationship for morphine-induced increase in slope conductance.
Data were obtained from the steady-state voltage changes in control and during application of 10 μM morphine for >3 min. As shown from the intersection of the control and morphine curves for this neuron, the reversal potential for morphine was -74 mV.

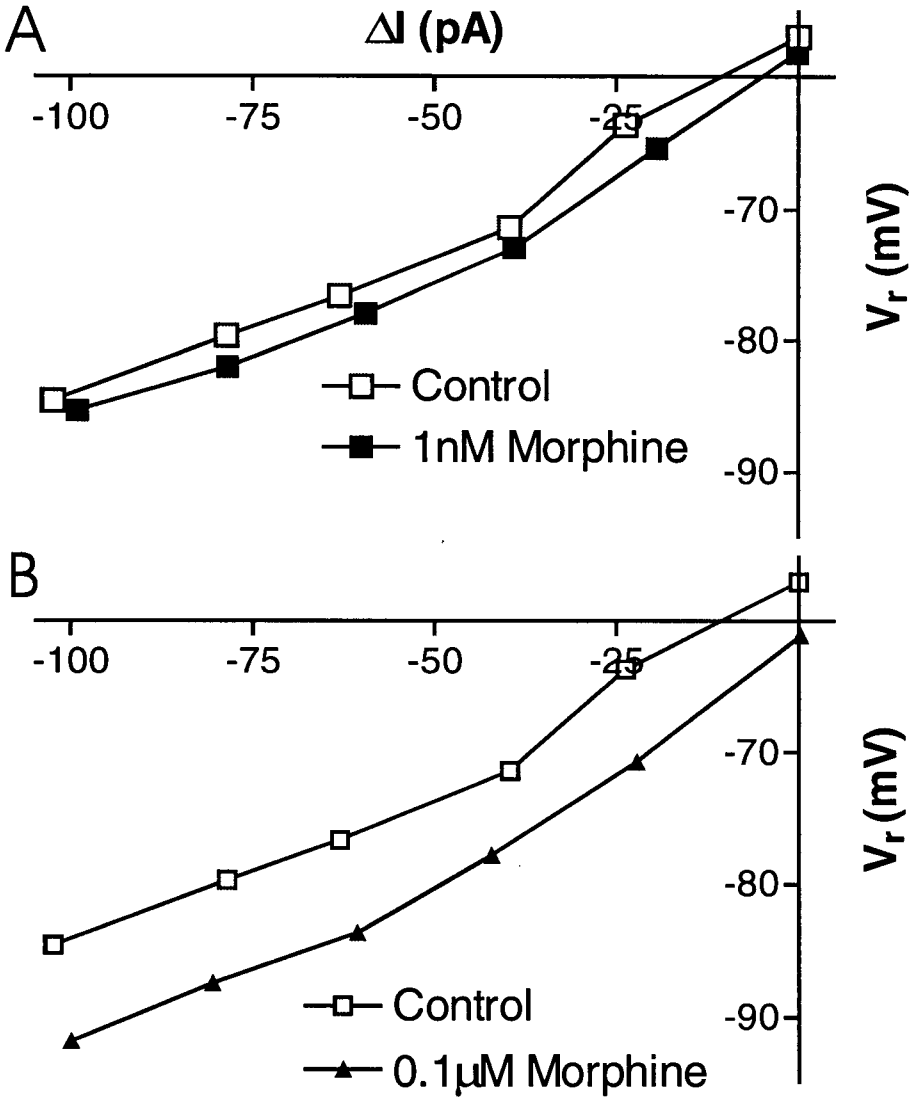

Fig. 3.10. Current-voltage relationship for morphine-induced decrease in slope conductance.
Data from neuron of Fig. 3.3. The responses were obtained during a cumulative application of morphine (0.1 nM to 0.1 μM). 1nM of morphine decreased the initial input conductance by 35 %, calculated from the exact values. Application of morphine decreased the slope conductance at potentials depolarized to V_r = -80 mV in 1 nM (A) and to V_r = -85 mV in 0.1 μM (B).

3.4 Effects of morphine during tetrodotoxin (TTX) blockade

The administration of TTX (300-600 nM) blocked action potentials in 71% of neurons (12 out of 17 neurons; Fig 3.11.A) and reduced the voltage responses to depolarizing current pulses. Application of TTX diminished the responses to hyperpolarizing current pulses in 59% of neurons (10 out of 17 neurons). The average increase of G_i was 28.7 ± 9.0 %, normalized to the initial input G_i (n = 10). Application of TTX caused an apparent increase in the slope conductance, calculated from steady-state voltage responses to subthreshold current pulses (Fig. 3.11.B). The remaining 41 % of neurons exhibited a decreased G_i, averaging 16.6 ± 3.6 % to the control response, when tested with hyperpolarizing current pulses. Application of TTX did not greatly affect V_r. The mean change in the V_r was ~1 mV, i.e., near the limits of detection (1.3 ± 0.5 mV, n = 17).

When applying TTX (300-600 nM) to block action potential-induced transmitter release, the application of morphine continued to increase or decrease the G_i (Fig. 3.12). The effects of morphine on G_i remained irreversible. Compared to the typical responses illustrated in Fig. 3.3, morphine had different effects on G_i during concomitant TTX application. In the absence of TTX and with hyperpolarizing current pulses, morphine at 10^{-6} M and 10^{-7} M, increased or decreased G_I (Fig. 3.3.A). However, during TTX application, morphine at the same concentrations, induced a decrease in G_i. The effects of morphine on G_i were smaller when depolarizing current pulses were used. Note that in the neuron of Fig. 3.13.A, the responses measured with depolarizing current pulses do not seem to depend on the morphine concentration.

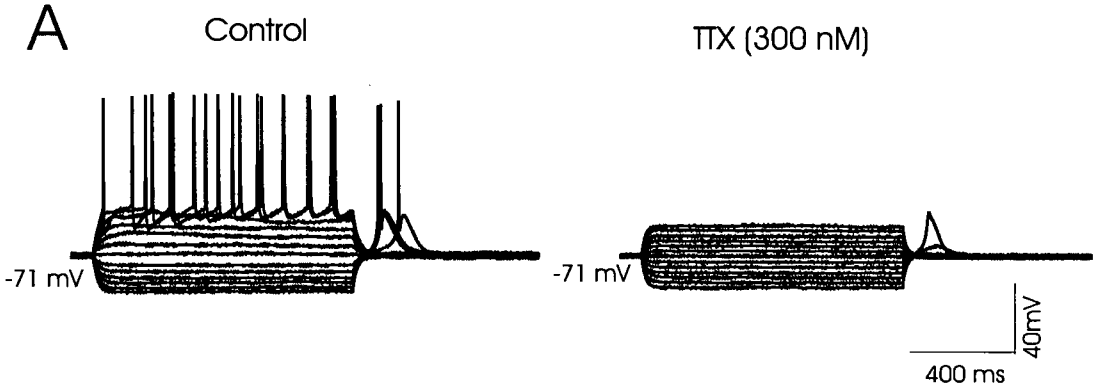

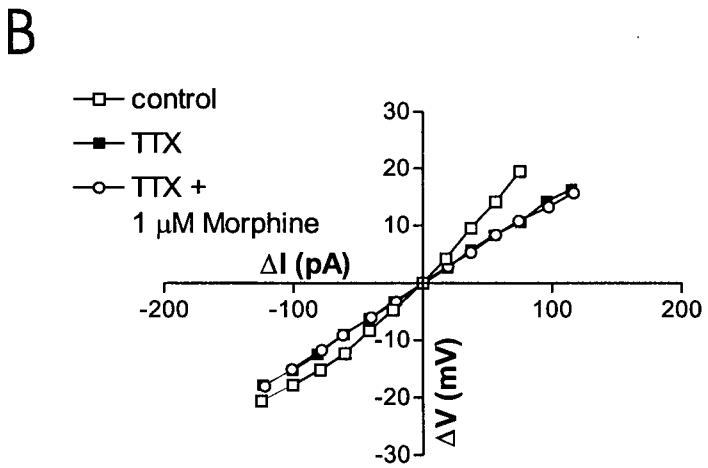

Fig. 3.11. Effects of TTX.
A: Application of TTX (300nM) for longer than 5 min, abolished tonic firing. The neuron was held at -71 mV. Under both conditions, the same current was injected. The current-voltage relationship is show in B. B: 5 min application of TTX (300 nM) reduced the slope conductance. The input conductance increased by 75 %. The subsequent application of morphine did not change the slope conductance.

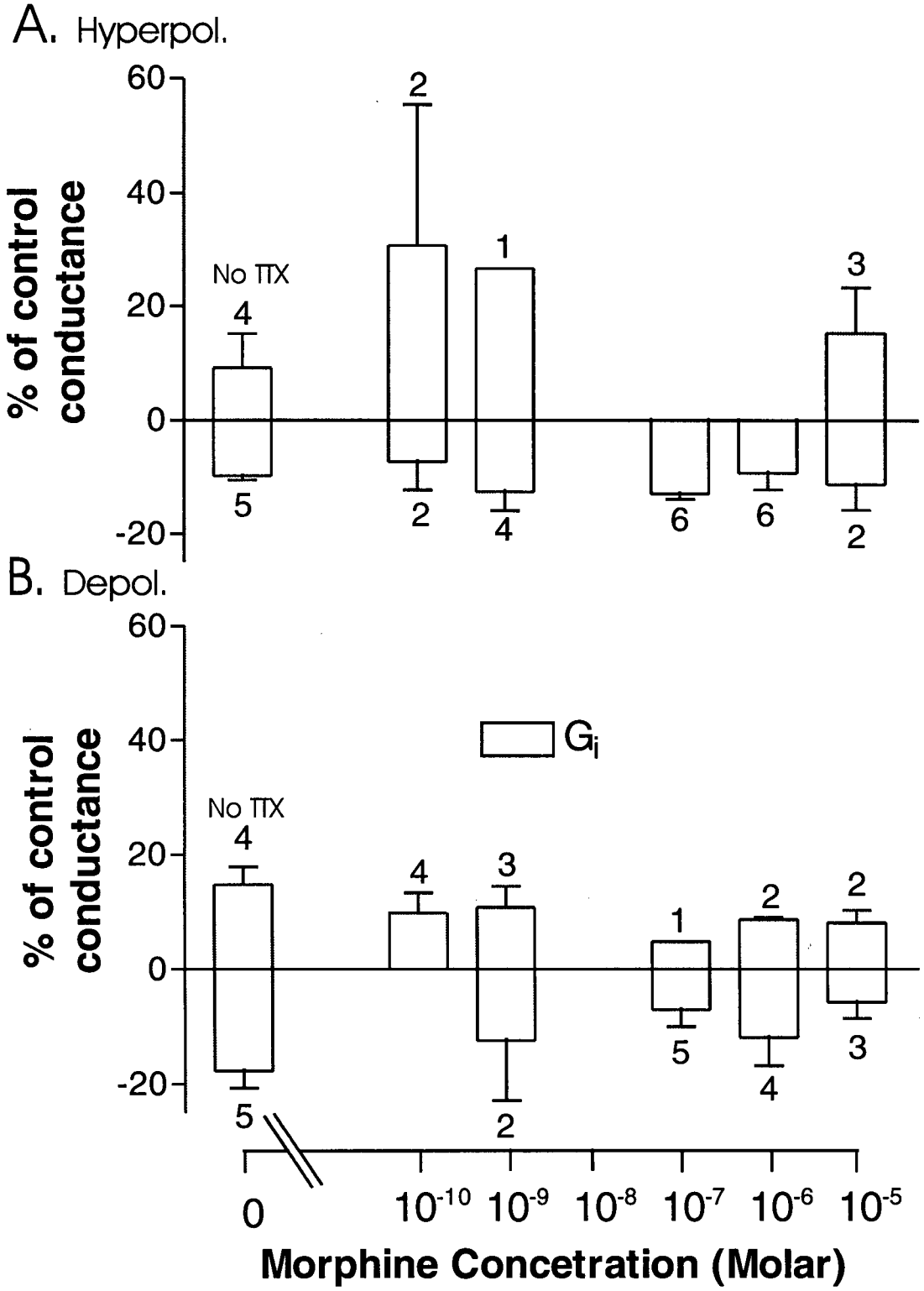
A. Hyperpol.
% of control conductance
60
40
20
0
-20
No TTX
4
5
2
2
1
4
6
6
3
2
B. Depol.
% of control conductance
60
40
20
0
-20
Gi
No TTX
4
5
4
2
3
2
1
5
2
4
2
3
0
10-10
10-9
10-8
10-7
10-6
10-5
Morphine Concetration (Molar)

Fig. 3.12. Effects of morphine on input conductance (G_i) during tetorodotoxin (TTX) application. (previous page)
For each neuron, the change in G_i was normalized to the initial input G_i. Application of morphine began more than 8 min after establishing a whole-cell configuration. TTX (300-600 nM) was applied until action potentials were no longer evoked in response to injecting depolarizing current pulses at ~100 pA morphine was then applied cumulatively. G_i in TTX was considered as a control value. A: Responses to injected hyperpolarizing current pulses. No TTX was applied during G_i measurements at the zero morphine concentration. Different from Fig. 3.3.A, in the 10^{-6} and 10^{-7} group, the change in G_i decreased in all neurons. At 10^{-10} M, the large mean response was due to the large increase in G_i by one neuron. B: Responses to injected depolarizing current pulses. The responses were not dependent on the morphine concentration.

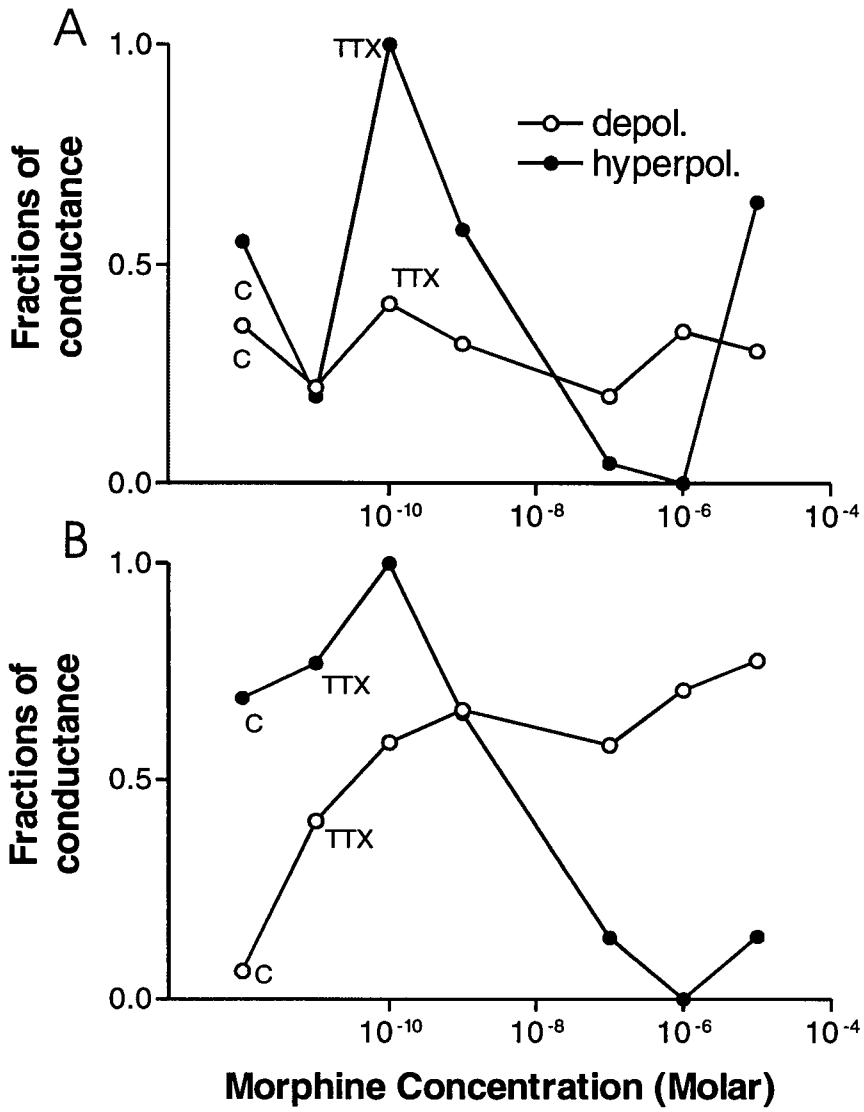

Fig. 3.13. Effects of morphine on input conductance (G_i) with tetorodotoxin (TTX) in cumulative application.

Two examples from Fig. 3.12 for the effects of cumulative application of morphine on the G_i determined from responses to injections of depolarizing and hyperpolarizing current pulses. For each neuron, all G_i were normalized by fractions, regarding the largest G_i as 1.0 and the smallest G_i as 0. C stands for the control value and TTX stands for the G_i after action potentials were completely abolished by TTX application (300-600 nM). In both neurons, the responses to hyperpolarizing current pulses yileded similar curves. In Fig. 3.11. A., the responses by depolarizing current pulses were independent of the morphine concentration.

Table 3.2. Effects of morphine on membrane potential (V_r) in neurons during action potential blockade with tetrodotoxin.

Increased G_i

Morphine Concentration (Molar)	ΔV_r (mV)	n
10^{-10}	0.0	2
10^{-9}	0.0	2
10^{-5}	-1.67 ± 1.20	3

Decreased G_i

Morphine Concentration (Molar)	ΔV_r (mV)	n
10^{-10}	-2.00 ± 1.00	2
10^{-9}	-1.00 ± 1.00	3
10^{-7}	-1.83 ± 0.60	6
10^{-6}	-1.92 ± 0.64	6
10^{-5}	-1.00 ± 0.00	2

During application of TTX, morphine hyperpolarized V_r in all neurons (n = 6; Table 3.2). The change in the V_r (ΔV_r) was smaller than the ΔV_r observed in the absence of TTX. Compared to changes measured at 0 μM morphine, one may assume that the changes in the V_r are independent of the morphine concentration.

In summary, the responses evoked by morphine application were modified by TTX. The effects of morphine did not necessarily result from actions only on the postsynaptic membrane.

3.5 Effects of morphine on firing patterns

In most neurons, morphine application decreased the just-threshold responses evoked by current pulses (1000 ms, duration). The changes in V_{thr} were associated with a decreased G_i (Fig. 3.14B), not an increased G_i (Fig. 3.14A). At a morphine concentration of 10^{-5} M, however, the action potential threshold increased by an average of ~2.5 mV. In neurons where morphine decreased G_i, the magnitude of reduced threshold was roughly proportional to the magnitude of to the G_i decrease, except at the higher concentrations of morphine (Fig. 3.14B).

Morphine application typically decreased the amplitude of the action potential (AP; Figs. 3.15A and 3.15B). In cases where morphine increased G_i, dose-dependent change in AP was similar to the dose-dependent change in G_i. In cases where morphine decreased G_i, the magnitudes of the AP change were not correlated to the magnitudes of change in G_i ignoring the largest change at 10^{-6} M (Fig. 3.15B).

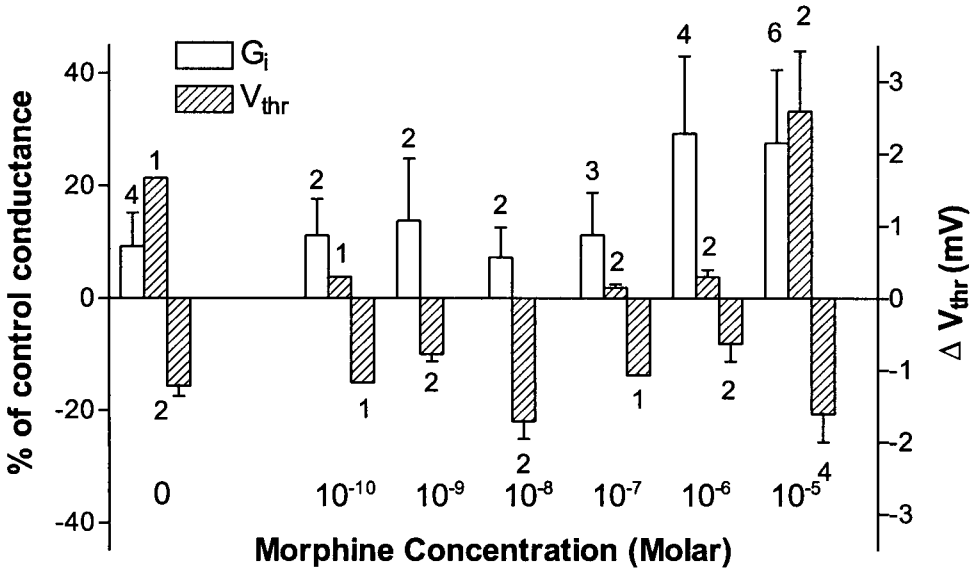

Fig. 3.14A. Relationship of morphine-induced increase in input conductance (G_i) to thresholds for action potential firing (V_{thr}). The V_{thr} was "just-threshold", defined at the amplitude of injected current that evoked the action potentials, approximately 50% of the time during successive current pulses (1000 ms, duration). The V_{thr} decreased at most concentrations of morphine. However, application of 10^{-5} M morphine produced biphasic changes in V_{thr} which significantly increased and then decreased.

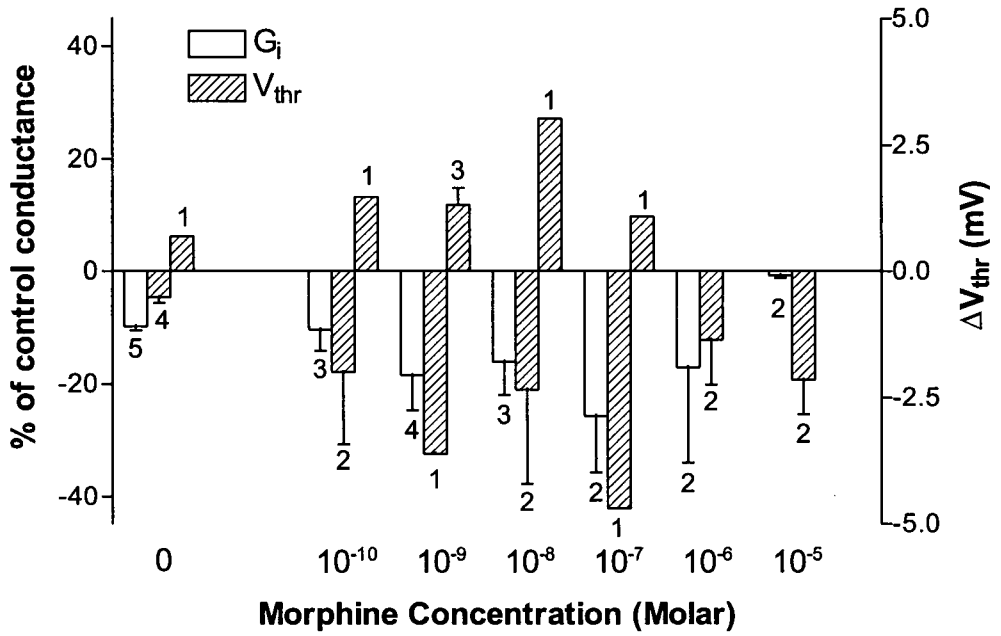

Fig. 3.14B. Relationship of morphine-induced decrease in input conductance (G_i) to threshold for action potentials (V_{thr}).
The V_{thr} decreased in most neurons. In most cases, the amount of decrease in V_{thr} is correlated to the concomitant decrease in G_i.

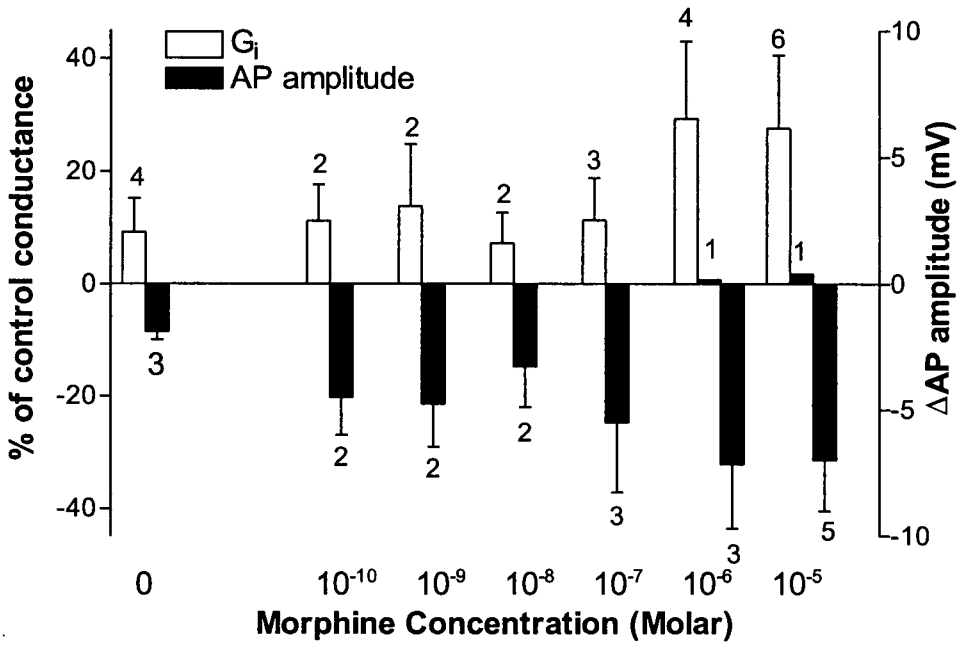

Fig. 3.15A. Relationship of morphine-induced increase in input conductance (G_i) to action potential (AP) amplitude.
Morphine application decreased the AP amplitude in most neurons. The changes in the AP (ΔAP) were greater at higher concentrations and corresponded to changes in G_i.

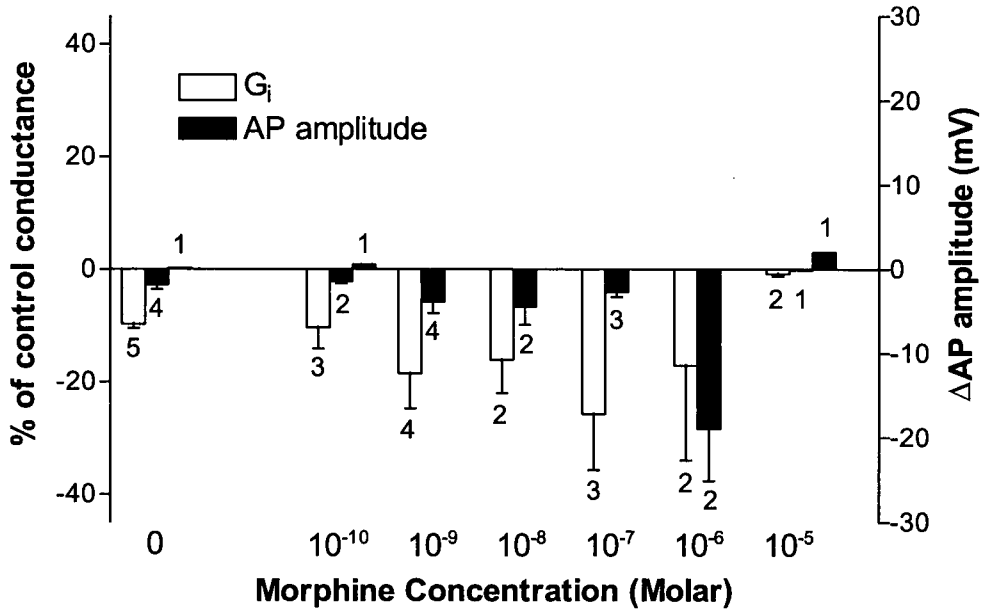

Fig. 3.15B. Relationship of morphine-induced decrease in input conductance (G_i) to action potential (AP) amplitude.
Morphine application decreased the AP in most neurons. Unlike changes in the AP found with the increased G_i, there is no association between the change in G_i and in AP.

Morphine application had little effect on spike half-width (Table 3.3) which reflects the roles of Na^+-currents and K^+-currents in the respective ascending and descending phases of the action potential. I separately analyzed spike duration either as a whole, or as a latter half width. Application of morphine at 10^{-6} M prolonged mean spike half-width, according to these criteria. However, the changes were not significant. Hence, I could not elucidate morphine's effects on the different ion activity in action potentials.

Morphine application changed the firing frequency and latency to the first spike evoked by current pulses (1000 ms, duration). Figure 3.16 illustrates three distinct examples of the changes. In pattern A, morphine application decreased the firing frequency or prolonged the latency to the first spike. In pattern B, morphine had no effect. In pattern C, morphine administration increased the firing frequency and shortened the latency to the first spike. The changes were not closely correlated with the change in the G_i. Even so, in the morphine-increased G_i category, >85 % of neurons showed pattern A or B (n = 24) and in the morphine-decreased G_i category, ~70% of neurons showed pattern B or C (n = 17).

In order to study morphine's effects on the spike afterhyperpolarization (AHP) through participation of Ca^{2+}-dependent K^+ currents, it was necessary to select data from neurons exhibiting the same firing frequency, i.e., for a comparison of control and morphine data. Unfortunately, I could not find enough data to satisfy this criterion.

The slow AHP is responsible for the alteration of firing properties in adaptation (Foehring et al. 1989). Most neurons (70%) showed spike-frequency

Table 3.3. Effects of morphine on spike-half width

Whole half width

Morphine Concentration (Molar)	control (ms)	morphine (ms)	n
0	2.49 ± 0.18	2.56 ± 0.18	8†
10^{-10}	2.67 ± 0.10	2.82 ± 0.15	5
10^{-9}	2.60 ± 0.11	2.67 ± 0.20	6
10^{-8}	2.67 ± 0.14	2.59 ± 0.40	5
10^{-7}	2.60 ± 0.086	2.76 ± 0.11	5
10^{-6}	2.67 ± 0.35	3.03 ± 0.22	6
10^{-5}	2.54 ± 0.26	2.73 ± 0.33	8

Latter half width

Morphine Concentration (Molar)	control (ms)	morphine (ms)	n
0	1.77 ± 0.14	1.84 ± 0.11	8†
10^{-10}	1.80 ± 0.065	1.85 ± 0.079	5
10^{-9}	1.76 ± 0.066	1.74 ± 0.13	6
10^{-8}	1.80 ± 0.065	1.68 ± 0.25	5
10^{-7}	1.75 ± 0.055	1.82 ± 0.026	5
10^{-6}	1.87 ± 0.28	1.97 ± 0.15	6
10^{-5}	1.84 ± 0.18	1.82 ± 0.22	8

† At 0 μM of morphine, the data were obtained from three different neurons.

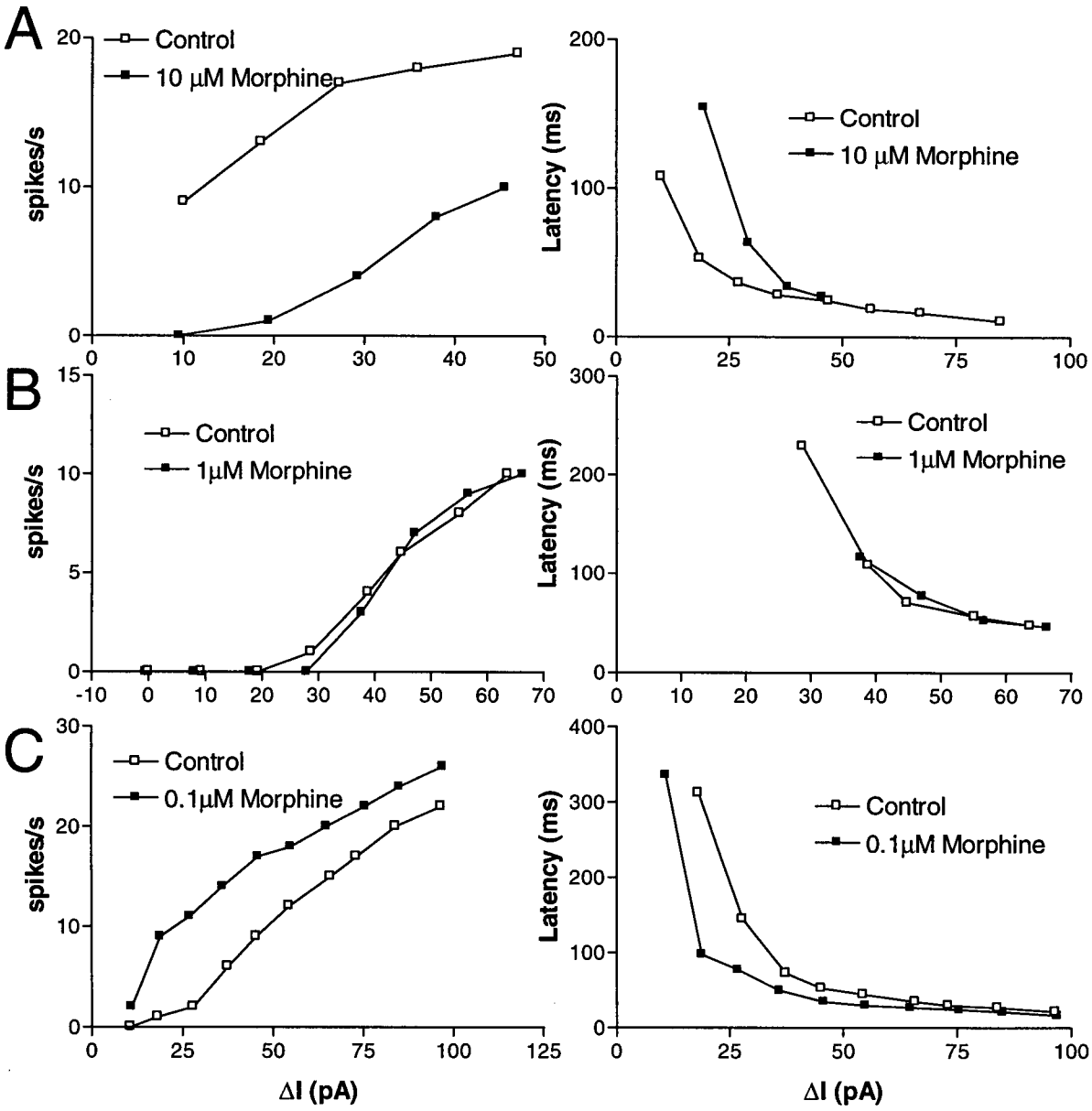
A
Control
10 μM Morphine
spikes/s
Latency (ms)
B
Control
1μM Morphine
spikes/s
Latency (ms)
C
Control
0.1μM Morphine
spikes/s
Latency (ms)
ΔI (pA)
ΔI (pA)

Fig. 3.16. Effects of morphine on firing frequency and latency to the first spike. (previous page)
Three example patterns for effects of morphine on firing frequency and latency to the first spike to square current pulses (1000 ms, duration). In the increased input conductance, for the firing rate, 46 %, 38 %, 16 % of neurons, and for the first spike latency, 68 %, 29 %, 3 % of neurons showed pattern A, B, C, respectively (n = 24). In the decreased input conductance, for the firing rate, 24 %, 35%, 41 %, and for the latency to the first spike, 24 %, 41 %, 35 % of neurons showed pattern A, B, C, respectively (n = 17).

adaptation in MGB (n = 10; Fig. 3.17). I measured the time between peaks of action potentials and used them for an inter-spike interval (ISI) analysis. Figure 3.17 shows a plot of spike-frequency that is the reciprocal of the ISI against the event of interval number. When the spike-frequency was >25 Hz, fast and slow phases were evident (Fig. 3.17.A). By comparing the responses to the same current pulses, morphine application reduced the fast and slow phases, as well as the spike-frequency (Fig. 3.17.A and Fig. 3.17.B). The reduction of the spike-frequency adaptation was more obvious in a comparison of data at the same spike frequencies (Fig. 3.17.B).

3.6 Mu-opioids

Mu-opioid receptors are abundant in the MGB. The effects of a selective μ-opioid receptor agonist, DAMGO, were similar to that of morphine. I applied DAMGO at concentrations of 1 nM to 0.1 μM in both Groups 1 and 2 (n = 12; data not shown). Application of DAMGO increased and decreased the G_i, hyperpolarizing the V_r to values between 0 and >5 mV. Other investigators demonstrated the reversible effects of DAMGO in thalamic neurons (Bruton and Charpak, 1998). However, I did not observe reversal of the effects after 30 s applications of DAMGO, despite observation periods of 30 min. The reversal potential for DAMGO was –69.5 ± 11.5 mV (n = 2), which was similar in value to that for morphine in Group 2. Therefore, I conclude that morphine activated μ-opioid receptors in MGB neurons.

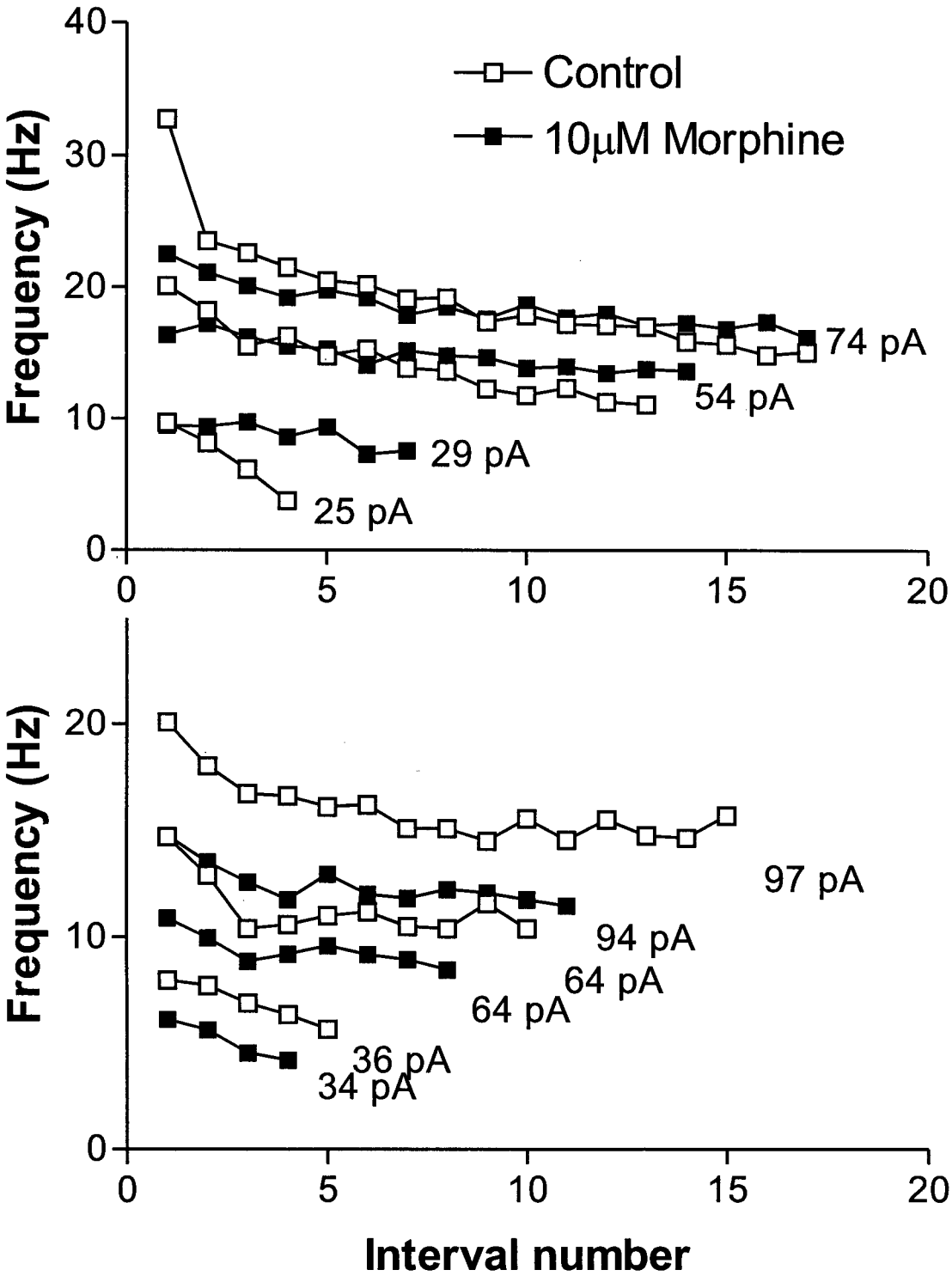
Control
10μM Morphine
Frequency (Hz)
40
30
20
10
0
74 pA
54 pA
29 pA
25 pA
0
5
10
15
20
Frequency (Hz)
20
10
0
97 pA
94 pA
64 pA
64 pA
36 pA
34 pA
0
5
10
15
20
Interval number

Fig. 3.17. Effects of morphine on spike-frequency adaptation. (previous page)
Spike frequency (1/inter-spike interval) vs. the interval number. Each trace is a response to injected pulse currents (1000 ms, duration) which is shown in right-side of the trace. 70 % of neurons showed spike-frequency adaptation, which had a fast phase and a slower phase. When the frequency was over 25 Hz, the fast phase was observed. Morphine application reduced the frequency and blocked both fast and slower phases. In B, the second trace of control in response to 64 pA and the first trace with 10 μM of morphine in response to 94 pA are the identical firing rate. The reduction in spike-frequency adaptation is clear in fast phase.

3.7 Blockade by naloxone

Naloxone blocked the effects of morphine in a time-dependent manner. As described above, a washing with ASCF did not reverse the effects of 0.01 to 0.1 μM morphine or 1 nM to 0.1 μM DAMGO. When the wash was longer than 20 min, a subsequent application of 1-10 μM of naloxone (3-10 min) did not reverse the change in the G_i (Fig. 3.18; n = 4).

Conversely, a naloxone application that started within 20 min after terminating opioid application, counteracted both the opioid induced increase and decrease of G_i (Fig. 3.19; n = 4). By itself and prior to co-application with morphine, naloxone evoked a small decrease in G_i. When co-applied with morphine, naloxone opposed the effects of morphine. In Fig. 3.19, for example, the G_i was increased by morphine and then decreased by a delayed application of naloxone. This reversal, likely antagonism, was observed in the absence and presence of TTX.

Application of naloxone as a pretreatment blocked the effects of morphine or DAMGO (n = 11). For this procedure, I first applied naloxone (10 μM) for 5-20 min which, alone, did not greatly alter V_r (-0.4 ± 0.5 mV; n = 10), but when applied for ~5 min, either increased G_i by 18.1 ± 6.3 % (n = 8) or decreased G_i by 25.4 ± 5.5 % (n =3). I applied either morphine (0.1 μM) or DAMGO (0.1 μM) while continuing the naloxone application (10 μM) for an additional 3 min. Then, the naloxone application terminated was and opioid application was continued. Despite either the naloxone-induced increase or decrease in G_i, naloxone reversed the effects of the opioids on V_r and G_i (Fig. 3.20). Note the differing durations of naloxone pretreatment in Figure 3.20. Also, the blockade of opioid action by naloxone was dependent on the

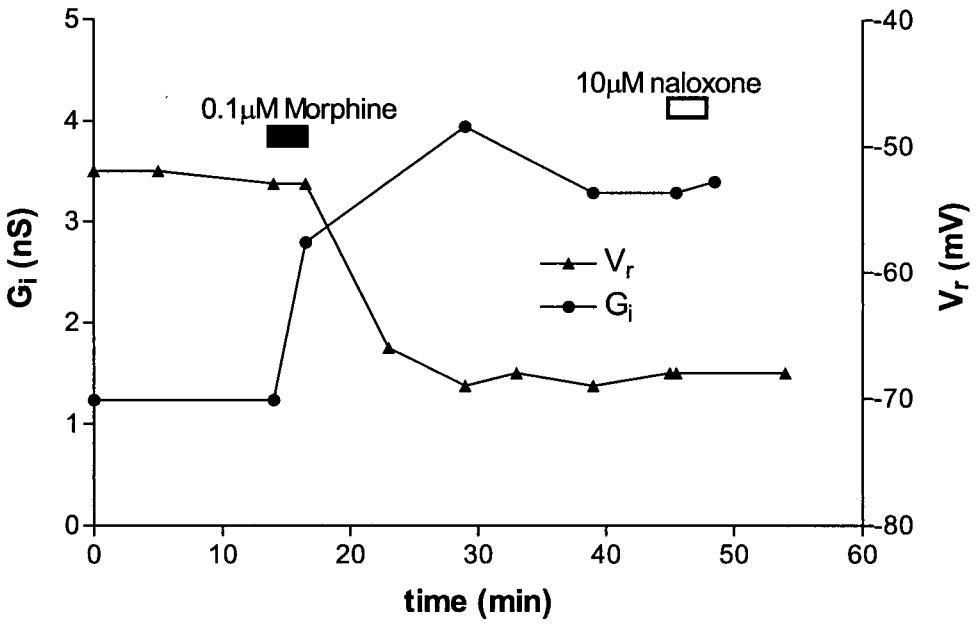

Fig. 3.18. Effects of morphine and naloxone on input conductance (G_i) and membrane potential (V_r).
The graph shows the effects of morphine and naloxone of the same neuron as in Fig. 3.2. An application of morphine (10 μM) for 3 min significantly increased the G_i and decreased the V_r. These effects were not reversible, despite termination of the morphine application for 24 min. A subsequent application of naloxone (10 μM) for 3 min did not reverse these effects of morphine.

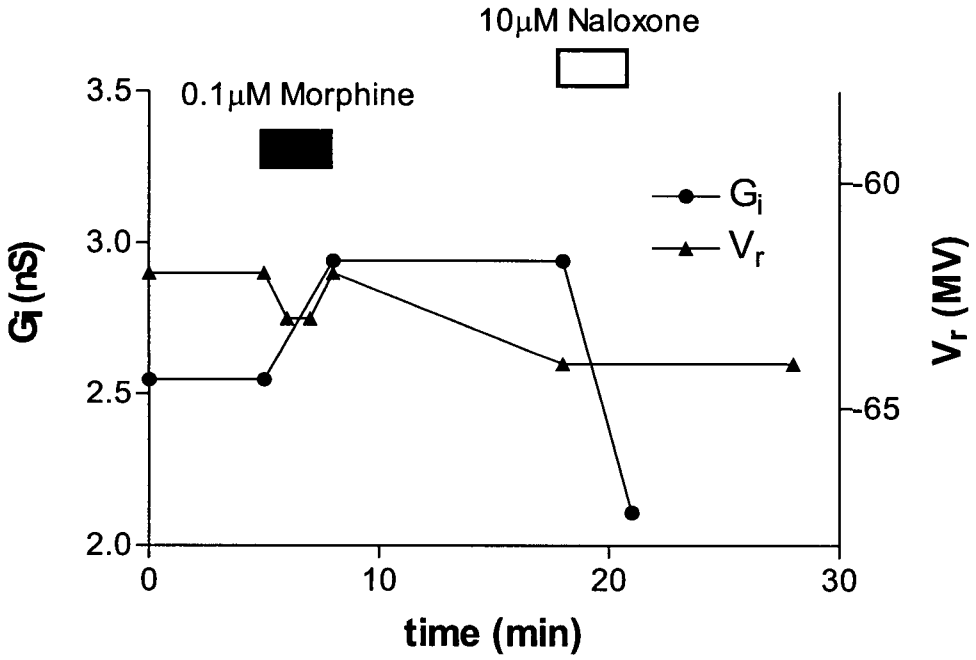

Fig. 3.19. Antagonistic action of a delayed application of naloxone to morphine on input conductance (G_i) and membrane potential (V_r).

0.1 μM of morphine application (3 min) increased the input G_i by 15.5 % and hyperpolarized the V_r temporarily and hyperpolarized by 2 mV before starting naloxone application. Brief hyperpolarization might be due to changing solution from control to morphine. Delayed application of naloxone (10 μM, 3 min) antagonized the effects of morphine on the G_i. The G_i with naloxone was smaller than the G_i in control by 17.3 %.

duration of naloxone application. The prior application of naloxone did not reverse the effects of a later application of an opioid applied for 5-10 min (Fig. 3.20.A). When naloxone pretreatment only slightly affected V_r and G_i (see above) and its application time was >15 min, a combined application of naloxone and opioid did not result in changes in G_i and V_r. However, application of opioid counteracted the effects of naloxone pretreatment when the antagonist produced either an increase or decrease in G_i (Fig. 3.20.B).

3.8 Blockade by Ba^{2+}

My previous experiments demonstrated that K^+-currents are involved in activation by morphine. If only K^+-conductances were increased by morphine application, V_r would hyperpolarize due to an increased G_i. Previous investigators have reported that Ba^{2+} blocked K^+-currents activated by morphine and other μ-opioids in thalamic and locus coeruleus neurons (North and Williams 1985; Bruton and Charpak 1998). To determine the participation of such currents in the responses to morphine, I used Ba^{2+}, as well as TTX to block transmitter-release. After completely abolishing action potentials with TTX, I applied Ba^{2+} (200 μM) for >12 min prior to morphine application. Ba^{2+} application (with TTX) depolarized the neurons by 6 mV to 11 mV, reaching a plateau value after >12 min (n = 8). From a V_r near –60 mV, Ba^{2+} decreased G_i more when measured with hyperpolarizing, than with depolarizing pulses. Ba^{2+} decreased the G_i by ~60 % and unmasked a sag in the voltage response, as previously observed (Fig. 3.21A; Tennigkeit et al. 1996). At this point, I assumed that Ba^{2+} blocked a substantial portion of the K^+ currents and

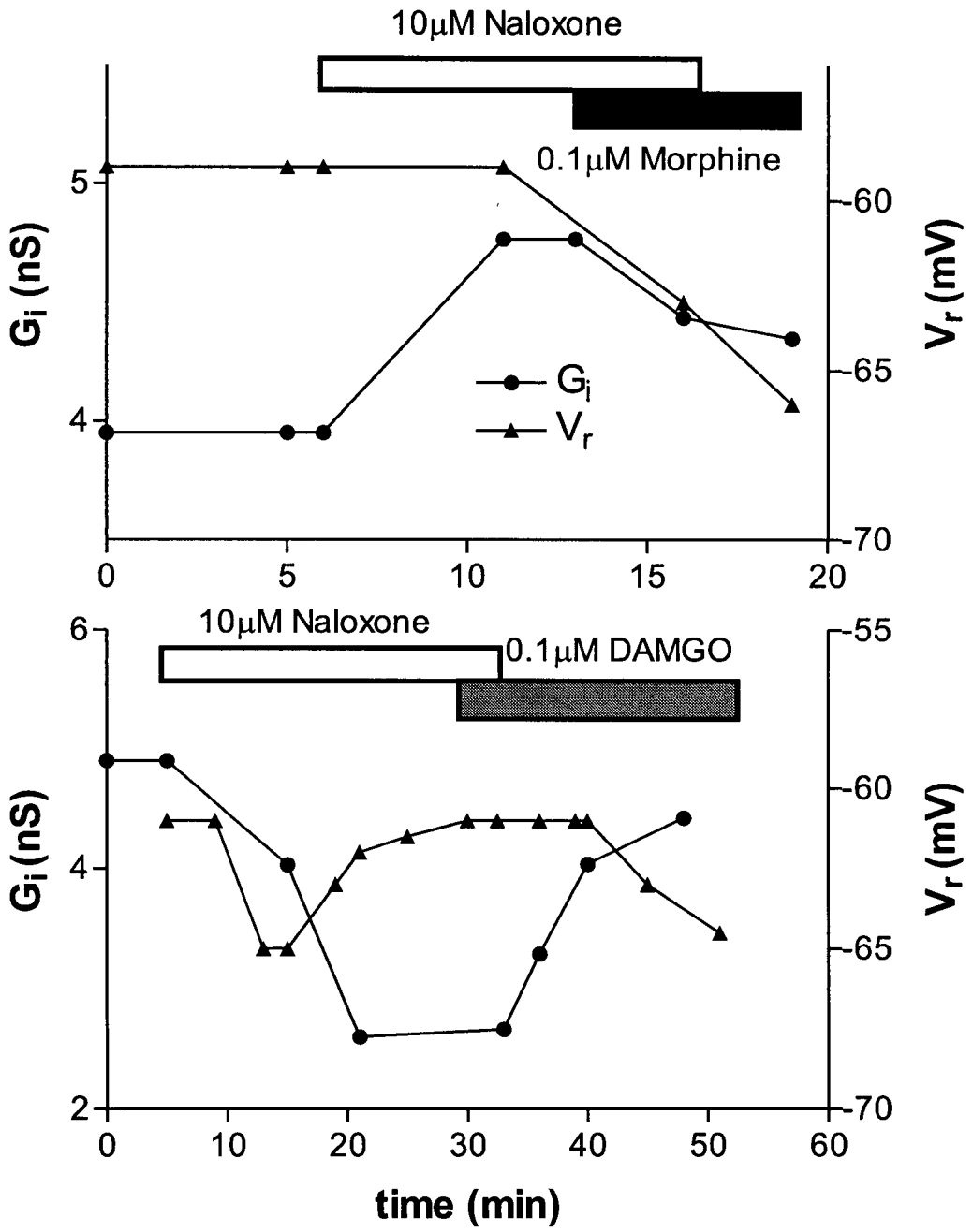
10μM Naloxone
0.1μM Morphine
G_i (nS)
V_r (mV)
G_i
V_r
10μM Naloxone
0.1μM DAMGO
time (min)

Fig. 3.20. Reversed effects of advance application of naloxone to opioids on input conductance (G_i) and membrane potential (V_r). (previous page)

A: 7 min advance application of naloxone could not reverse the effects of morphine. Naloxone application (10 μM) increased the G_i by 20.7 % and did not change the V_r. Combined application of naloxone and morphine (0.1 μM) decreased the G_i and the V_r. Morphine application alone continued the combined effects. B: 20 min advance application of naloxone could antagonize the effects of DAMGO. Application of naloxone (10 μM) decreased the input G_i. The V_r was hyperpolarized briefly when naloxone application was started and recovered to the control level during the application of naloxone. Combined application of naloxone and DAMGO (0.1 μM) did not change the G_i and the V_r. Only DAMGO application increased the G_i and hyperpolarized the V_r. Note different time scales in A and B.

co-applied morphine. Cumulative application of morphine from 10^{-9} to 10^{-5} M produced a greater reduction in G_i with depolarizing, than with hyperpolarizing current pulses (n = 6; Fig. 3.21B). In Fig. 3.20B, the changes in G_i were greatest with pulses in both directions at 10^{-7} M and became smaller with hyperpolarizing current pulses at 10^{-5} M. This feature was also observed in an absence of Ba^{2+} (Fig 3.13). With or without co-application of Ba^{2+}, the greatest changes in G_i occurred at morphine concentrations of 10^{-9} M in 4 neurons, 10^{-7} M in 3 neurons and 10^{-6} M in 3 neurons. These effects do not apparently involve I_{NaP} and may be a consequence of morphine acting on I_H (see Discussion).

Furthermore, higher concentrations of morphine increased the amplitude of the LTS in response to hyperpolarizing current pulses (>–100 pA; Fig. 3.21A). A 10 to 15 min wash with TTX-containing ASCF reversed these effects.

Application of Ba^{2+} blocked the effects of morphine and unmasked a sag in the voltage responses to hyperpolarizing pulses. These effects, accompanied by a depolarization of 8 to 11 mV, were apparent if Ba^{2+} was applied either before, or after morphine. In the presence of TTX, application of morphine (0.1 to 10 μM) increased G_i (Figs. 3.22A and 3.22B). This change in the G_i was reversed by a subsequent application of Ba^{2+} (0.2 to 1 mM). A thorough washing with TTX-containing ASCF for 30 min reversed these effects.

TTX

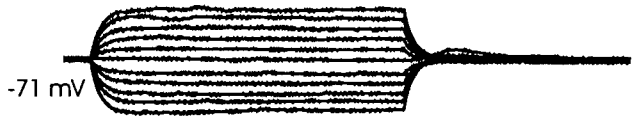

TTX + Ba^{2+}

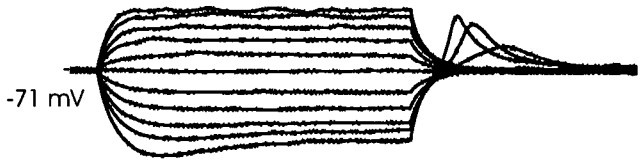

TTX + Ba^{2+} + 10 μM Morphine

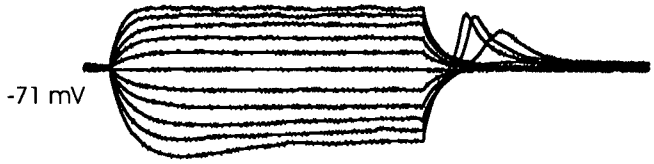

Wash

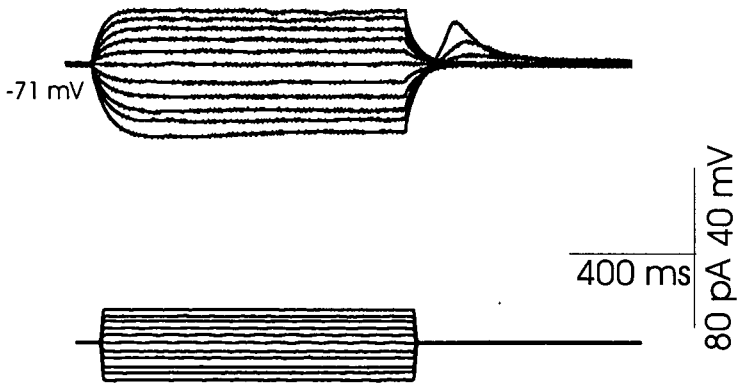

Fig. 3.21A. Effects of Ba^{2+} on morphine response. (previous page)
After blocking action potentials by TTX, Ba^{2+} (200 μM) was applied for 12 min. Application of Ba^{2+} increased the input resistance and unmasked a sag in the voltage response. Co-application of 10 μM of morphine had little effect on the input resistance. Morphine application hightened low threshold Ca^{2+} spike to hyperpolarizing current pulses. These effects were reversible.

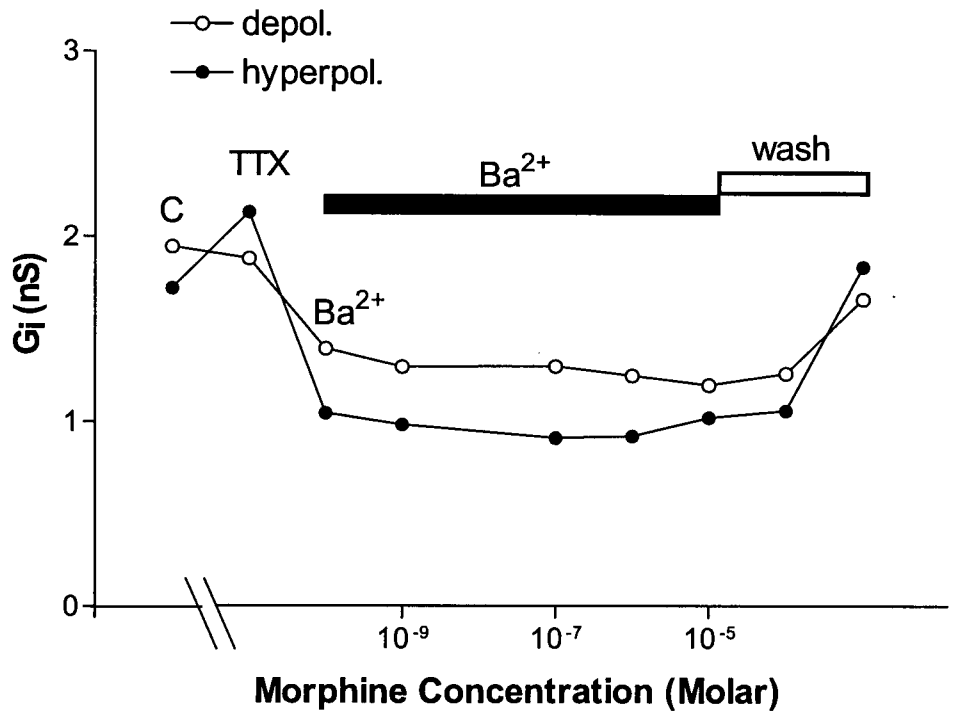

Fig. 3.21B. Effects of Ba^{2+} on cumulative application of morphine. After action potentials were abolished by TTX (300-600 nM), Ba^{2+} (200 μM) was applied for 12 min. The G_i was calculated from the voltage response to ~10 pA depolarizing and hyperpolarizing current pulses. From 10^{-9} to 10^{-5} M of morphine did not change G_i in the presence of Ba^{2+}.

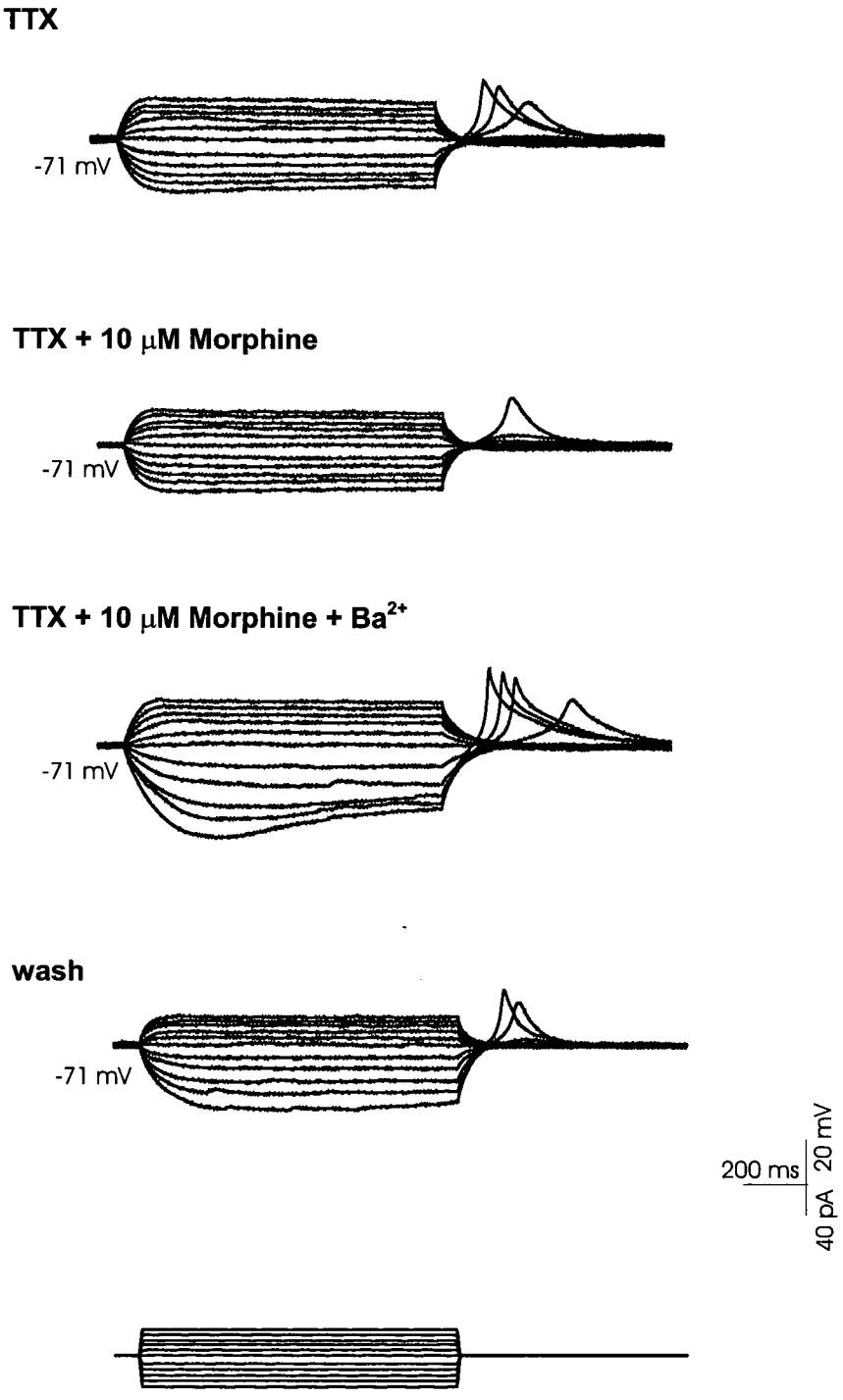
TTX
-71 mV
TTX + 10 μM Morphine
-71 mV
TTX + 10 μM Morphine + Ba2+
-71 mV
wash
-71 mV
200 ms
20 mV
40 pA

Fig. 3. 22A. Effects of Ba^{2+} on morphine response. (previous page) After blocking action potentials with TTX, 10 μM morphine (3 min) increased G_i. Ba^{2+} blocked the effects of morphine and decreased G_i more than the control G_i. Ba^{2+} application unmasked a sag in the voltage record. These effects were reversed by washing.

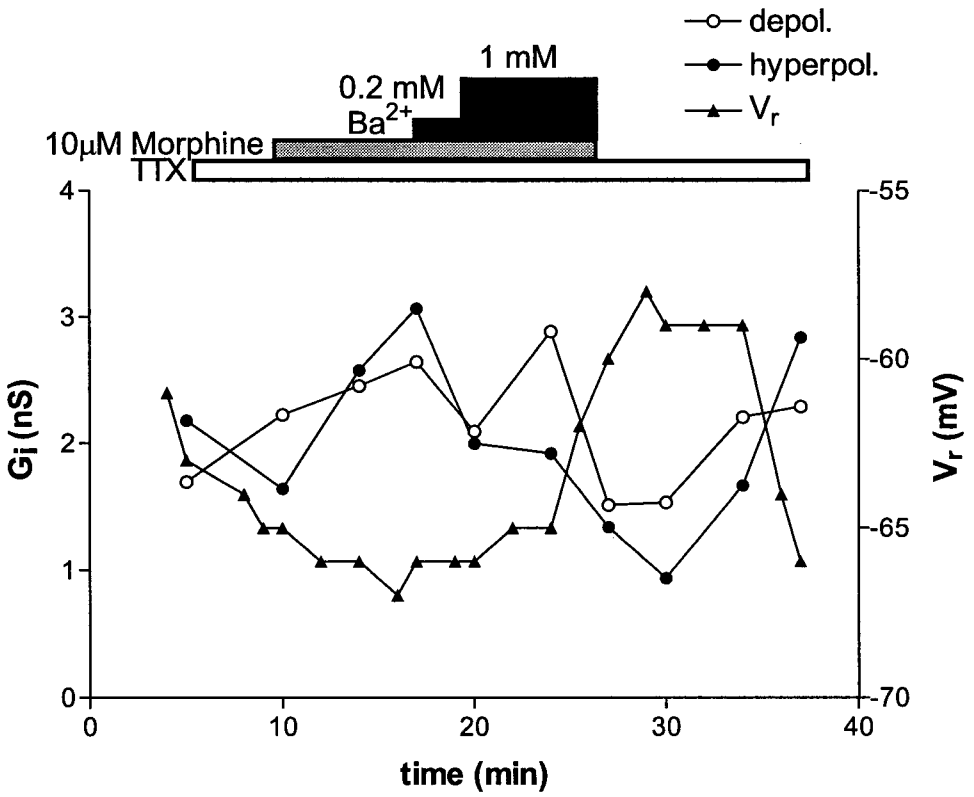

Fig. 3.22B. Ba^{2+} acts in a concentration-dependent manner to alter morphine responses.
In TTX, 10 μM morphine application increased G_i. Subsequent application of Ba^{2+} (0.2 mM) did not change the V_r. After Ba^{2+} was increased to 1 mM, Ba^{2+} blocked the effects of morphine and decreased G_i below control G_i. V_r depolarized 8 mV. These effects were reversed by washing.

3.9 Effect of low-Na^+

To elucidate the mechanism of morphine's greater effect on the voltage responses to hyperpolarizing, than depolarizing pulses, I performed experiments where we substituted NMDG for Na^+, a major ion carried by I_H channel. I changed the extracellular [Na^+] from 150 mM to 26 mM, using NMDG.

I perfused low Na^+-ACSF containing TTX before and after morphine application (n = 2). The low [Na^+] ACSF hyperpolarized V_r by 6 mV and decreased G_i by 25-35 % (Fig. 3.23) and reduced the changes in V_r and G_i during morphine application. A co-application of TTX and Ba^{2+} appear to make clearer, the effects of low [Na^+] on morphine-induced changes in V_r and G_i.

The effects of morphine on the persistent Na+ current ($I_{Na,P}$) were investigated on one neuron. We held this neuron at –71 mV and, at –51mV where $I_{Na,P}$ likely would be more than 50% activated. Before starting morphine application, NMDG application for 12 min decreased G_i as revealed by hyperpolarizing current pulses from 1.64 nS to 0.71 nS, just after stopping the NMDG application. At –71 mV, NMDG application reduced the morphine-induced change in the G_i (1 μM), where as there was reduction when the neuron was held at –51 mV.

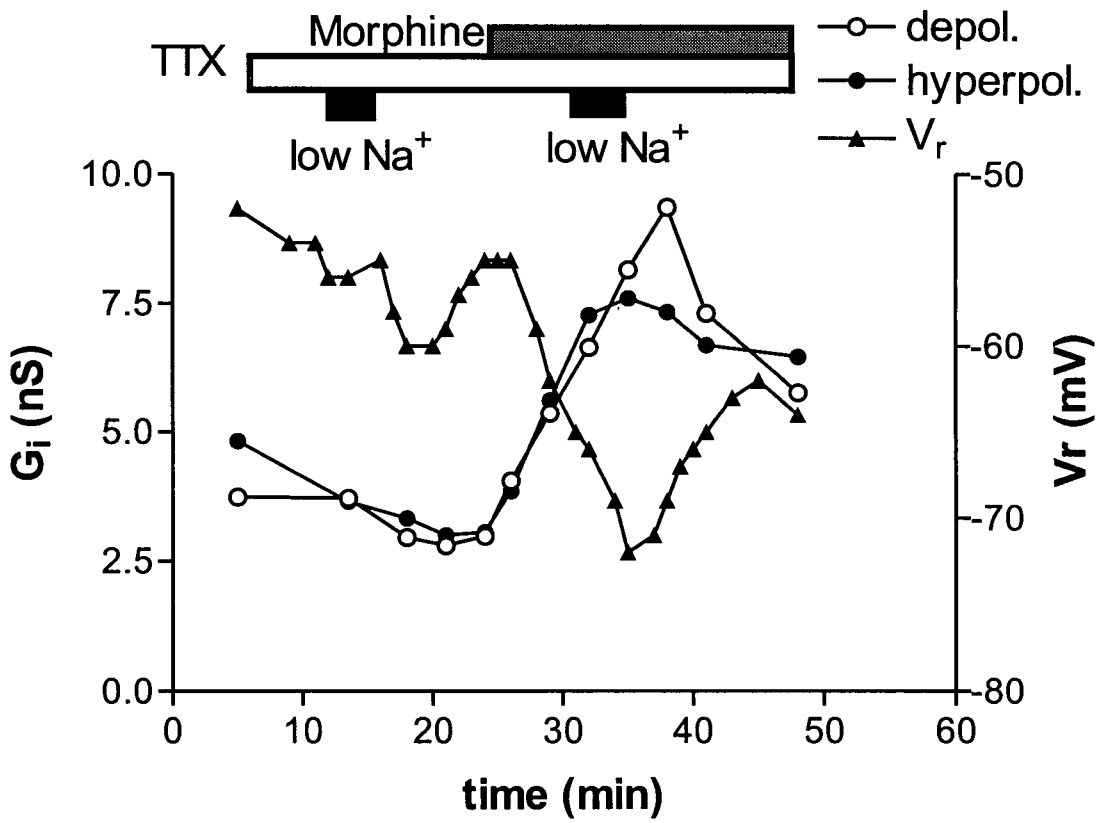
TTX
Morphine
low Na+
low Na+
depol.
hyperpol.
Vr
10.0
7.5
5.0
2.5
0.0
Gi (nS)
-50
-60
-70
-80
Vr (mV)
0
10
20
30
40
50
60
time (min)

Fig. 3.23. Effects of low-Na^+ to morphine on input conductance (G_i) and membrane potential (V_r). (previous page)
In the presence of TTX (300 nM), we changed extracellular Na^+ from 150 mM to 26 mM for 3 min before and after 10^{-8} M morphine application. Without morphine application, exchanging extracellular solution hyperpolarized V_r and decreased G_i in response to both depolarizing and hyperpolarizing current pulses. During morphine application, the change in V_r and G_i were smaller.

4. Discussion

In these experiments, I have examined the effects of morphine and DAMGO on membrane conductance and spike firing at gerbil MGB neurons. I observed both increases and decreases in membrane conductance. The increased input conductance may be due to an increased K^+ conductance, whereas the decreased conductance may have resulted from a blockade of the hyperpolarization activated inward current, I_H. The application of morphine, a μ and δ opioid agonist, and DAMGO, a μ selective opioid agonist, had similar effects. From their reversal potentials, I suggest that, their activation of μ receptors produced the effects through similar ionic mechanisms. Naloxone antagonized these effects, consistent with opioid effects on MGB neurons being mediated via opioid receptors. It now remains to briefly summarize these results and provide feasible explanations for these effects.

4.1 Influence of gerbil age on membrane properties and action potentials

Compared to other studies in thalamic nuclei, the V_r and R_i observed here were relatively high and τ_m was longer than in previous studies (Tennigkeit et al. 1996; Williams et al. 1996). These characteristics are repesentative of thalamocortical neurons from younger animals (Ramoa and McCormick 1994; Tennigkeit et al. 1998). In our studies, 20% of the neurons did not display an evoked LTS. However, Tennigkeit et al. (1998) observed only two such neurons in >P14 animals. In their studies, this may have resulted from the selection of neurons from only the ventral partition of the MGB. With respect to the action potential (AP),

V_{thr}, AP amplitude, and AP duration had almost identical values to those from adult neurons (Ramoa and McCormick 1994; Tennigkeit et al. 1998). Hence, the characteristics of the AP achieve maturity earlier than the other membrane properties (Ramoa and McCormick 1994).

Several studies have shown differential development of membrane ionic channels, pumps or transporters. For example, tetraethlyammonium (TEA) sensitive K^+ channels have a role in determining the duration of action potentials in P26 neurons, but not in P3-5 neurons (Spigelman et al. 1992). V_r is largely dependent on the Na^+-K^+ pump activity, which develops significantly after P14 (Molnar et al. 1999). Thus, the disparity in the development of ionic channels and pumps may account for the different rate of maturity of membrane properties, reversal potentials and firing modes in younger animals versus older animals. In summary, we cannot assume that membrane properties remain homogeneous in neurons sampled experimentally in animals aged P9 to P16 days.

4.2 Effects of morphine on passive and active membrane properties

The largest differences in the effects of experiment 1 and experiment 2 were changes in G_i. We conducted these experiments in two ways: (1) observations in neurons starting >8 minutes after break-through (Group 1) and (2) observations in neurons starting >3 minutes after break-through (Group 2). The large increase in the conductance in Group 2 might have resulted from mechanical damage of the neuronal membrane after its perforation and the equilibration of its contents with internal pipette solution (Ries and Puil 1999). Since morphine application time was

the same between Group 1 and Group 2, the involvement of a second messenger system by morphine is an unlikely cause for the large increase in the G_i in Group 2.

The effects of morphine and DAMGO were not reversed on washout in the present study. There are no studies on opioid effects in MGB neurons. However, in other neurons (Cherubini et al. 1984) and in rat thalamic neurons (Bruton and Charpak 1998), morphine or DAMGO effects are reversed with washing. Moreover, in my studies, a subsequent application of naloxone did not reverse the effects of morphine and DAMGO when the wash was longer than 20 min. The absence of recovery cannot be attributed to a short control period, e.g., in Group 2, where the control value might have changed before starting morphine application, since the effects of opioid application were also not reversed in Group 1. The absence of reversibility may reflect a second messenger system activation by the opioid. Opioid receptors are members of the G-protein coupled-receptor family (Uhl et al. 1994).

Morphine and DAMGO application changed G_i. Differences in activating currents at membrane potentials between ~—50 mV and ~-70 mV may have induced the different responses to depolarizing and hyperpolarizing current pulses. Below, I will discuss, in more detail, the effects of depolarizing and hyperpolarizing current pulses. The morphine concentration-response relationship for G_i showed no statistical significant difference between each concentration (Fig. 3.5). The failure to find a significant effect might be due to the mixed action of the opioids. I separated the conductance changes into increased and decreased groups for each concentration of morphine (Figs. 3.4 and 3.5). In each concentration group (Fig. 3.5), responses were mixed, ranging from 1 % to 89%. The smaller change in G_i

may have resulted from a balance between opioid evoked opening and closing of ion channels. It also remains possible that not all of the MGB neurons express opioid receptors to some extent (see Ding et al. 1996).

The large difference in conductance between Group 1 and Group 2 influenced the morphine concentration-response curves (Figs. 3.4.A and 3.5). In Group 2, it was difficult to determine an EC_{50}. Although Fig.3.4.A shows concentration-response curves without TTX that are different from other opioid studies, the responses to hyperpolarizing current pulses (Fig.3.4.A) in cases where DAMGO increased G_i, yielded similar curves and EC_{50} values in thalamic centrolateral neurons (Bruton and Charpak 1998) and guinea pig nodose ganglionic neurons (Ingram and Williams 1994). Hence, the control value in Group 2 is probably inaccurate and more time should be allowed after break-through to the whole-cell configuration, before taking measurements.

The changes in G_i coupled with the changes in V_r, evoked by morphine and DAMGO application are consistent with the activation of more than one type of ion channel. At higher concentrations of morphine, G_i increased and V_r decreased. This might represent increases in K^+ and Cl^- conductances. A more positive holding current was needed to maintain the same potential after applying morphine and the morphine induced increase in G_i was blocked by Ba^{2+}. These findings are consistent with hypothesis that the change in G_i resulted from opioid activation of an outward K^+ current. At lower morphine concentrations, the increased G_i, coupled with the increased V_r, may reflect opioid activation of Ca^{2+} or Na^+ currents or the hyperpolarization activated inward current, I_H. Opioids induce increases in

intracellular Ca^{2+} concentration (Jin et al. 1992; Tang et al. 1996) and also shift the activation curve of I_H along the voltage-axis to more negative potentials (Ingram and Williams 1994). At lower concentrations of morphine, there was a tendency for G_i and V_r to decrease. In such cases, morphine application might block K^+ ion channels or the Na^+-K^+ pumps. Morphine application itself is a known enhancer of Na^+-K^+ pump activity (Sykoba et al. 1985). Hence, when opioids decreased G_i and V_r, it seems possible that the opioid blocked K^+ channels or maintenance of the $[K^+]$ gradient. When opioids decreased G_i and increased V_r, they may have blocked an inward current. However, I observed such actions only on two neurons.

In summary, opioid application appears to increase K^+ conductance at higher concentrations and to decrease a K^+ conductance, Na^+-K^+ pump activity or activation of I_H, at lower concentrations. Finally, the initial R_i had no correlation to either the increase or decrease in G_i evoked by opioid application. From these data, I suggest that opioid activates K^+ channels as well as other ion channels.

A change in membrane capacitance (C_m) could account for morphine's action on τ_m. The increase in G_i coupled with the change in τ_m, occurred only at lower concentration of morphine. Thus far, two studies have shown that opioids can alter C_m (Rusin et al. 1997; Sargent et al. 1988). However, they demonstrated that κ-opioid receptors, but not μ- and δ-opioid receptor activation altered C_m. These might reflect methodological and experimental differences. Sargent et al. (1998) used a model membrane and Rusin et al. (1997) used rat neurohypophysial endings, which have a high density of κ-opioid receptors and a low density of μ- and δ-opioid receptors (Mansour et al. 1994). Rusin et al. (1997) used three different opioid

agonists at 1-3 μM, a concentration at which I also observed little effect on C_m. Hence, it remains possible that μ-opioids have an effect on C_m.

When G_i increased, the reversal potential was between –61 mV and –67 mV, strongly implying that opioids activate K^+ channels along with other ion channels in MGB neurons. When the G_i decreased, opioid actions did not reverse in the voltage range from ~-100 mV to ~-50mV. In my experiments, the calculated reversal potential for K^+ is –85 mV and for Cl^- is –58 mV. This implies that cationic currents are involved in the activation of currents by opioids in MGB neurons.

TTX application altered the morphine concentration-response curve, compared to morphine application alone (Fig. 3.4 and Fig. 3.12). This implies that the action of morphine has an effect at presynaptic sites. In the presence of TTX, morphine application still had effects on the G_i, but did not greatly change V_r. Opioids may activate Cl^- channels with an equilibrium potential near V_r, or the sum resulting from different changes in G_i to various ions equals 0 mV.

Opioids are inihibitory at presynaptic sites (Johnson and North 1993). These inhibitory effects are mediated by diminishing Ca^{2+}-activated presynaptic transmitter release. Johnson and North (1993) suggested that opioids act on voltage-gated Ca^{2+} channels to reduce Ca^{2+} influx, resulting in a reduction of transmitter release. So far, there is no report that opioid acts on Cl^- channels. Nevertheless, it is plausible that morphine application in the presence of TTX activates several ion channel types.

In the presence of TTX, I observed different responses to depolarizing and hyperpolarizing current pulses (Fig. 3.13). The difference is more obvious in the

presence of Ba^{2+}. From –70 mV to –50 mV, the change in voltage activates and inactivates several ion channels, which might induce the distinctive actions to depolarizing versus hyperpolarizing current pulses. With hyperpolarizing current tests, G_i decreased whereas G_i was unchanged when the neurons were tested with depolarizing current pulses. Such effects are consistent with morphine inhibiting I_H. Several investigators have demonstrated the blockade of I_H by opioids in the locus coreruleus, nodose ganglion and hippocampus (Alreja and Aghajanian 1993; Ingram and Williams 1994; Svoboda and Lupica 1998). The different G_i responses to depolarizing and hyperpolarizing current pulses were concentration-dependent; the responses were largest at 10^{-9} to 10^{-7} M of morphine concentration. Thus, a hyperpolarizing shift of I_H might occur primarily at relatively lower concentration of opioids in MGB neurons.

4.3 Effects of opioids on firing properties

Opioid application decreased AP amplitude, depending on the magnitude of the increased G_i and the concentration. Similarly, a recent study has shown that extracellular application of morphine reduced the peak Na^+-current in a concentration-dependent manner in rat and human cardiac myocytes (Hung et al. 1998). In their study, application of morphine did not change the Ca^{2+} current, outward current, or inwardly rectifying K^+ current. Therefore, Hung et al. (1998) concluded that the morphine inhibits a Na^+ current in myocytes. However, in our study, morphine application appeared to have effects on K^+ and other currents. Morphine may have inhibited directly, or shunted the Na^+- currents.

Opioid application did not have significant effects on spike-half amplitude. An increase in Na^+ conductance comprises the first half part of the AP, and K^+ channels are involved in the latter half of the AP. The absence of effects imply that opioid application has no blocking actions on spike-generating Na^+ channels or the delayed rectifier responsible for repolarization. Spigelman et al. (1992) demonstrated that in mature rat hippocampal neurons, TEA, but not 4-aminopyridine (4-AP), application prolonged spike duration. If we postulate that our neurons contain similar currents as in their experiments, opioid application did not affect TEA-sensitive or 4-AP-insensitive K^+-currents, such as inward rectifiers or several Ca^{2+}-activated K^+ channels.

In the case where morphine decreased G_i, there was little change in the AP, except at 10^{-6} M of morphine. Morphine application did not significantly reduce action potential amplitude compared to sham applications. Hence, the reduction observed in action potential might be due to cell deterioration. Since I have data from only two neurons at 10^{-6} M, it is difficult to infer any effect.

Morphine may block Ca^{2+}-activated K^+ channels. Unfortunately, we could not get enough data to analyze the spike afterhyperpolarization (AHP), mediated by a Ca^{2+}-activated K^+ conductance. Instead, I examined spike-frequency adaptation, in part resulting from activated Ca^{2+}-mediated K^+ channels. Unlike rat MGB neurons (Tennigkeit et al. 1998), we observed spike-frequency adaptation in gerbil MGB neurons. In addition, similar to cortical neurons (Foehring et al. 1989) or motoneurons (Kernell 1965), the adaptation had an early fast phase and late slower phase and is not observed in other thalamocortical neurons (Ramoa and McCormick

1994). Blockade of spike-frequency adaptation by morphine application indicates that morphine inhibits Ca^{2+}- or Na^{+}-mediated K^{+} currents (Foehring et al. 1989). Ca^{2+}-mediated K^{+} channels have three subtypes (reviewed by Sah 1999). Apamine insensitive Ca^{2+}-mediated K^{+} channels have a role in spike-frequency adaptation because of their slow activation. In addition, this channel might regulate the AHP, together with small conductance Ca^{2+}-mediated K^{+} channels, which are apamine-sensitive.

Opioid actions have paradoxical effects on the AHP. In guinea pig myenteric plexus cells, morphine prolonged the AHP, following a train of action potentials (Tokimasa et al. 1981; Cherubini et al. 1984). In the rat dorsal root ganglion, several opioid agonists blocked the tail currents following depolarizing current pulses, which are mediated by Ca^{2+}-activated K^{+} channels (Akins and McCleskey 1993). However, in guinea pig or rabbit coeliac ganglion neurons, morphine did not inhibit the slow AHP (Cassell and McLachlan 1987). The coeliac ganglion neurons demonstrate enkephalin immunoreactivity. Cassell and McLachlan (1987) used higher concentrations of morphine, compared to other studies, showing the blocking effects on Ca^{2+}-activated K^{+} channels. Hence, blockade of Ca^{2+}-activated K^{+} channels by morphine might be tissue dependent.

Opioid application induced contradictory effects on spike-frequency adaptation and on the excitability of neurons. Blockade of apamine-insensitive Ca^{2+}-activated K^{+} channels reduces spike-frequency adaptation and increases the excitability of the neuron. However, we observed opioid application blocked spike-frequency adaptation and reduced the firing frequency when morphine increased G_i.

Lidocaine application in the thalamic neurons also induced the same contradictory effects (Schwarz and Puil 1998). As explained before by Schwarz and Puil (1998), the contradictory effects might result from a shunt of Na^+ current. We observed the blockade of spike-frequency adaptation only at higher concentrations of morphine, when the G_i was increased in most neurons. This observation supports the shunt hypothesis.

4.4 Conclusion

I suggest that μ-opioid application has effects on several ion channels. My experiments demonstrate that opioids might reduce the activation of I_H at lower concentrations and increase the activation of K^+ currents at higher concentrations. As described in the Introduction, opioids have roles in both increasing and decreasing the excitability of thalamocortical neurons. The concentration-dependent dual action of opioids have been observed in mouse dorsal root ganglion (Crain and Shen 1990). From my experiments, I suggest that morphine has excitatory effects that occur at lower concentrations and swamp the effective inhibitory actions, which might explain opioid induce seizures.

5. References

AKINS, P.T. AND MCCLESKEY, E.W. Characterization of potassium currents in adult rat sensory neurons and modulation by opioids and cyclic AMP. *Neurosci.* 56(3): 759-769, 1993

ALREJA, M. AND AGHAJANIAN, G.K. Opiates suppress a resting sodium-dependent inward current and activate an outward potassium current in locus coeruleus neurons. *J. Neurosci.* 13(8): 3525-3532, 1993

AGHAJANIAN, G.K. AND RASMUSSEN, K. Intracellular studies in the facial nucleus illustrating a simple new method for obtaining viable motoneurons in adult rat brain slices. *Synapse* 3(4): 331-338, 1989

BELLGOWAN, P.S.F. AND HELMSTETTER, F.J. Neural systems for the expression of hypoalgesia during nonassociative fear. *Behav. Neurosci.* 110(4): 727-736, 1996

BLUMBERG, H., DAYTON, H.B., GEORGE, M. AND RAPAPORT, D.N. N-allylnoroxymorphone: a potent narcotic antagonist. *Fed. Proc.* 20: 311, 1961

BODNAR, R.J., WILLIAMS, C.L. LEE, S.J. AND PASTRENAK, G.W. Role of μ_1-opiate receptors in supraspinal opiate analgesia: a microinjection study. *Brain Res.* 477: 25-37, 1988

BUNZOW, J.R., SAEZ, C., MORTRUD, M., BOUVIER, C., WILLIAMS, J.T., LOW, M. AND GRANDY, D.K. Molecular cloning and tissue distribution of a putative member of the rat opioid receptor gene family that is not a mu, delta, or kappa opioid receptor type. *FEBS Lett.* 347(2-3): 284-288, 1994

BRUTON, J. AND CHARPAK, S. μ-opioid peptides inhibit thalamic neurons. *J. Neurosci.* 18(5), 1998

CASSELL, J.F. AND MCLACHLAN, E.M. Two calcium-activated potassium conductances in a subpopulation of celiac neurones of guinea-pig and rabbit. *J. Physiol.* 394: 331-349, 1987

CHALMERS, A., MCGEER, E.G., WICKSON, V. AND MCGEER, P.L. Distribution of glutamic acid decarboxylase in the brains of various mammalian species. *Comp. Gen. Pharmac.* 1: 385-390, 1970

CHAN-PALAY, V., ITO, M., TONGROACH, P., SAKURAI, M. AND PALAY, S. Inhibitori effects of motilin, somatostatin, [leu]enkephalin, [met] enkephalin, and taurine on neurons of the lateral vestibular nucleus: interactions with γ-aminobutyric acid. *Proc. Natl. Acad. Sci. U.S.A.* 79: 3355-3359, 1982

CHERUBINI, E., MORITA, K. AND NORTH, R.A. Morphine augments calcium-dependent potassium conductance in guinea-pig myenteric neurones. *Br. J. Pharmacol.* 81: 617-622, 1984

CHEN, Y., MESTEK, A., LIU, J., HURLEY, J.A. AND YU, L. Molecular cloning and functional expression of a mu-opioid receptor from rat brain. *Mol. Pharmacol.* 44(1): 8-12, 1993

CHILDERS, S.R. Opioid receptor-coupled second messenger systems. *Life Sci.* 48(21): 1991-2003,1991

CRAIN, S.M. AND SHEN, K.-F. Opioids can evoke direct receptor-mediated excitatory effects on neurons. *Trends Pharmacol. Sci.* 11, 77-81, 1990

DING, Y., KANEKO, T., NOMURA, S. AND MIZUNO, N. Immunohistochemical localization of μ-opioid receptors in the central nervous system of the rat. *J. Comp. Neurol.* 367:375-402, 1996

DUGGAN, A.W. AND NORTH, R.A. Electrophysiology of opioids. *Pharmacol. Rev.* 35(4): 219-281, 1983

EDWARDS, F.A., KONNERTH, A., SAKMANN, B. AND TAKAHASHI, T. Thin slice preparation for patch clamp recordings from neurones of the mammalian central nervous system. *Pflügers Arch.* 414: 600-612, 1989

FOEHRING, R.C., SCHWINDT, P.C. AND CRILL, W.E. Norepinephrine selectively reduces slow Ca^{2+}- and Na^{+}- mediated K^{+} currents in cat neocortical neurons. *J. Neurophysiol.* 61(2): 245-256, 1989

FOWLER, C.J. AND FRASER, G.L. μ-, δ-, κ-opioid receptors and their subtypes. A critical review with emphasis on radioligand binding experiments. *Neurochem. Int.* 24(5): 401-426, 1994

FRENK, H., MCCARTY, B.C. AND LIEBESKIND, J.C. Different brain areas mediate the analgesic and epileptic properties of enkephalin. *Science* 200: 335-336, 1978

FREY, H.H. AND VOITS, M. Effects of psychotropic agents on a model of absence epilepsy in rats. *Neuropharmacology* 30: 651-656, 1991

FREYE, E., LATASCH, L. AND PORTOGHESE, P.S. The delta receptor is involved in sufentanil-induced respiratory depression-opioid subreceptors mediate different effects. *Eur. J. Anaesthesiol.* 9(6): 457-462, 1992

GILBERT, P.E. AND MARTIN, W.R. The effects of morphine-, and nalorphine-like drugs in the non-dependent, morphine-dependent and cyclazocine-dependent chronic spinal dog. *J. Pharmacol. Exp. Ther.* 197(3): 517-532, 1976a

GILBERT, P.E. AND MARTIN, W.R. Sigma effects of nalorphine in the chronic spinal dog. *Drug Alcohol Depend.* 1(6): 373-6, 1976b

GOLDSTEIN, A. Interactions of narcotic antagonists with receptor sites. *Adv. Biochem. Psychopharmacol.* 8(0): 471-81, 1973

GRECO, B., PREVOST, J. AND GIOANNI, Y. Intracerebral microinjections of dermorphine: search for the epileptic induction thresholds. *Neuroreport* 5: 2169-2172, 1994

GRONROOS, M AND PERTOVAARA, A. A selective suppression of human pain sensitivity by carbon dioxide: central mechanisms implicated. *Eur. J. Appl. Physiol. Occup. Physiol.* 68(1): 74-9, 1994

HELMSTETTER, F.J. AND BELLGOWAN, P.S. Hypoalgesia in response to sensitization during acute noise stress. *Behav. Neurosci.* 108: 177-185, 1994

HENDERSON, G., MCKNIGHT, S. AND CORBETT A. 1999 Receptor & Ion Channel Nomenclature Supplement, *Trends Pharmacol Sci.*, 1999

HERZ, A. Peripheral opioid analgesia-facts and mechanisms. *Prog. Brain Res.* 110: 95-104, 1996

HO, J., MANNES, A.J., DUBNER, R., CAUDLE, R.M. Putative kappa-2 opioid agonists are antihyperalgesic in a rat model of inflammation. *J. Pharmacol. Exp. Ther.* 28: 1136-1142, 1997

HUGHES, J. Isolation of an endogenous compound from the brain with pharmacological properties similar to morphine. *Brain Res.* 88: 295-308, 1975

HUNG, C.F., TSAI, C.H. AND SU, M.J. Opioid receptor independent effects of morphine on membrane currents in single cardiac myocytes. *Br. J. Anaesth.* 81(6): 925-31, 1998

INGRAM, S.L. AND WILLIAMS, J.T. Opioid inhibition of I_h via adenylyl cyclase. *Neuron* 13: 179-186, 1994

JASINSKI, D.R., MARTIN, W.R. AND HAERTZEN, C.A. The human pharmacology and abuse potential of n-allylnoroxymorphone (naloxone). *J. Pharmacol. Exp. Ther.* 167(2): 420-426, 1967

JIN, W., LEE, N.M., LOH, H.H. AND THAYER, S.A. Dual excitatory and inhibitory effects of opioids on intracellular calcium in neuroblastoma × glioma hybrid NG 108-15 cells. Mol. Pharmacol. 42(6): 1083-1089, 1992

JOHNSON, S.W. AND NORTH, R.A. Presynaptic actions of opioids, in: Dunwiddie, T.V. and Lovinger, D.M. (Eds), *Presynaptic receptors in the mammalian brain*, Boston: Birkenhäuser: 71-76,1993

KANDEL, E.R., SCHWARTZ, J.H. AND JESSELL, T.M. The perception of pain, in: *Principles of neural science (fourth edition)*, McGraw-Hill: 473-506, 2000

KANJHAN, R. Opioids in pain. *Clin. Exp. Pharmacol. Physiol.* 22(6-7): 397-403, 1995

KEMP, J.A., FOSTER, A.C., WONG, E.H. AND MIDDLEMISS, D.N. A comment on the classification and nomenclature of phencyclidine and sigma receptor sites. *Trends Neurosci.* 11(9): 388-9, 1988

KERNELL, D. The adaptation and the relation between discharge frequency and current frequency and current strength of cat lumbosacral motoneurons stimulated by long-lasting injected currents. *Acta Physiol. Scand.* 65: 65-73, 1965

KNAPP, R.J., MALATYNSKA, E., FANG, L., LI, X., BABIN, E., NGUYEN, M., SANTORO, G., VARGA, E.J., HRUBY, V.J., ROESKE, W.R. AND YAMAMURA, H.I. Identification of a human delta opioid receptor: cloning and expression. *Life Sci.* 54(25): PL 463-468, 1994

KIRKUP, J. Surgery before general anesthesia. in: MANN R.D. (ed.). *The history of the management of pain.* Casterton Hall: Parthenon Publishing Group: 15-30, 1988

KUNGEL, M. AND FRIAUF, E. Somatostatin and leu-enkephalin in the rat auditory brainstem fetal and postnatal development. *Anat. Embryol.* 191: 425-443, 1995

LEE, R.L., MCCABE, R.T., WAMSLEY, J. K., OLSEN, R.W. AND LOMAX, P. Opioid receptor alterations in a genetic model of generalized epilepsy. *Brain Res.* 380: 76-82, 1986

LIN, Y. AND CARPENTER, D.O. Direct excitatory effects mediated by non-specific actions on rat medial vestibular neurons. *Eur. J. Pharmacol.* 262, 99-106, 1994

MANSOUR, A., FOX, C.A., BURKE, S. MENG, F., THOMPSON, R.C., AKIL, H. AND WATSON, S.J. Mu, delta, and kappa opioid receptor and mRNA expression in the rat CNS: an in situ hybridization study. *J. Comp. Neurol.* 350: 412-438, 1994

MANSOUR, A., FOX, C.A., AKIL, H. AND WATSON, S.J. Opioid-receptor mRNA expression in the rat CNS: anatomical and functional implications. *Trends Neurosci.* 18 (1): 22-29, 1995

MARTIN, W.R., EADES, C.G., THMPSON, J.A, HUPPLER, R.E. AND GILBERT, P.E. The effects of morphine and nalorphine-like drugs in the nondependent and morphine-dependent chronic dog. *J. Pharmacol. Exp. Ther.* 197(3): 517-532, 1976

MAYER, D.J., WOLFE, T.L., AKIL, H., CARDER, B. AND LIEBESKIND, J.C. Analgesia from electrical stimulation of the brain stem of the rat. *Science* 174: 1351-1354, 1971

MELDRUM, B.S., MENINI, C., NAQUET, R., RICHE, D. AND SILVA-COMTE. Absence of seizure activity following focal cerebral injection of enkephalins in a primate. *Regul. Pept.* 2: 383-390, 1981

MOLNAR, L.R., THAYNE, K.A., FLEMING, W.W. AND TAYLOR, D.A. The role of the sodium pump in the developmental regulation of membrane properties of cerebellar Prukinje neurons of the rat. *Brain Res. Dev. Brain Res.* 112: 287-291, 1999

NAGASAKA , H., AWAD, H. AND YAKSH, T.L.A. Peripheral and spinal actions of opioids in the blockade of the autonomic response evoked by compression of the inflamed knee joint. *Anesthesiology* 85(4): 808-816, 1996

NEAL, C.R., MANSOUR, A., REINSCHEID, R., NOTHACKER, H. CLIVELLI, O. AND WATSON, S.J.JR. Localization of orphanian FQ (nociceptin) peptide and messenger RNA in the central nervous system of the rat. *J. Comp. Neurol.* 406: 503-547, 1999

NISHI, M., HOUTANI, T., NODA, Y., MAMIYA, T., SATO, K. DOI, T., KUNO, J., TAKESHIMA, H., NUKADA, T., NABESHIMA, T., YAMASHITA, T., NODA, T. AND SUGIMOTO, T. Unrestrained nociceptive response and disregulation of hearing ability in mice lacking the nociceptin/orphanin FQ receptor. *EMBO J.* 16(8): 1858-1864, 1997

NORTH, R.A. AND WILLIAMS, J.T. On the potassium conductance increased by opioids in rat locus coeruleus neurones. *J. PHYSIOL.* 364: 265-280, 1985

OLAUSSON, B., ERIKSSON, E., ELLMARKER, L., RYDENHAG, B., SHYU, B.C. AND ANDERSSON, S.A. Effects of naloxone on dental pain threshold following muscle exercise and low frequency transcutaneuous nerve stimulation: a comparative study in man. *Acta Physiol. Scand.* 126(2): 299-305, 1986

PAPE, H.C., BUDDE, T., MAGER, R. AND KISVARDAY, Z.F. Prevention of $Ca(^{2+})$-mediated action potentials in GABAergic local circuit neurones of rat thalamus by a transient K^+ current. *J. Physiol.* 478 Pt 3: 403-422, 1994

PAPE, H.C. AND MCCORMICK, D.A. Electrophysiological and pharmacological properties of interneurons in the cat dorsal lateral geniculate nucleus. *Neuroscience* 68(4): 1105-25, 1995

PASTERNAK, G.W. Pharmacological mechanisms of opioid analgesics. *Clin. Neuropharmacol.* 16: 1-18, 1993

PAUL, D., PICK, C.G., TIVE, L.A. AND PASTERNAK, G.W. Pharmacological characterization of nalorphine, a κ_3 analgesic. *J. Pharmacol. Exp. Ther.* 257: 1-7, 1991

PERT, C.B. AND SNYDER, S.H. Opiate receptor: demonstration in nervous tissue. *Science* 179:1011-1014, 1973

PICK, C.G., ROQUES, B., GACEL, G. AND PASTERNAK, G.W. Supraspinal mu 2-opioid receptors mediate spinal/supraspinal morphine synergy. *Eur. J. Pharmacol.* 220(2-3): 275-7, 1992

POHL, J. Über das N-allylnorcodein, einen antagonisten des morphins. *Z. Exp. Pathol. Ther.* 17: 370-382, 1915

PRZEWŁOCKA, B., LASOŃ, W., TURCHAN, J., DE BRUIN, N., VAN LUIJTELAAR, G., PRZEWŁOCKA, R. AND COENEN, A. Anatomical and functional aspects of μ opioid receptors in epileptic WAG/Rij rats. *Epilepsy Res.* 29, 167-173, 1998

QUIRION, R., HAMMER, R.P. JR., HERKENMAN, M. AND PERT C.B. Phencyclidine (angel dust)/sigma "opiate" receptor: visualization by tritium-sensitive film. *Proc. Natl. Acad. Sci. U.S.A.* 78(9): 5881-5885, 1981

RAMOA, A.S. AND MCCORMICK, D.A. Developmental changes in electrophysiological properties of LGNd neurons during reorganization of retinogeniculate connections. *J. Neurosci.* 14(4): 2089-2097, 1994

REISINE, T. AND PASTERNAK, G. Opioid analgesics and antagonists. in: HARDMAN, J.G., LIMBIRD, L.E., MOLINOFF, P.B., RUDDON, R.W. AND GILMAN, A.G. (eds) *Goodman & Gilman's the pharmacological basis of therapeutics.* McGraw-Hill: 521-556, 1995

RIES, C.R. AND PUIL, E. Mechanism of anesthesia revealed by shunting actions of isoflurane on thalamocortical neurons. *J. Neurophysiol. 81*: 1795-1801, 1999

RUSIN, K.I., GIOVANNUCCI, D.R., STUENKEL, E.L. AND MOISES, H.C. κ-opioid receptor activation modulates Ca^{2+} currents and secretion in isolated neuroendocrine nerve terminals. *J. Neurosci. 17(17)*: 6565-6574, 1997

SAH, P. Ca^{2+}-activated K^{+} currents in neurones: types, physiological roles and modulation. *Trends Neurosci.* 19:150-154, 1996

SAHLEY, T.L. AND NODAR, R.H. Improvement in auditory function following pentazocine suggests a role in dynorphins in auditory sensitivity. *Ear Hear.* 15: 422-431, 1994

SARGENT, D.F., BEAN, J.W. AND SCHWYZER, R. Conformation and orientation of regulatory peptides on lipid membranes. Key to the molecular mechanism of receptor selection. *Biophys. Chem. 31(1-2)*: 183-193, 1988

SCHWARZ, S.K.F AND PUIL, E. Analgesic and sedative concentrations of lignocaine shunt tonic and burst firing in thalamocortical neurones. *Br. J. Pharmacol.* 124: 1633-1642, 1998

SIMON, E.J., HILLER, J.M. AND EDELMAN, I. Stereospecific binding of the potent narcotic analgesic ^{3}H etorphine to rat homogenate. *Proc. Natl. Acad. Sci. U.S.A.* 70: 1947-1949, 1973

SNYDER, S.H. Opiate receptors in the brain. *N. Engl. J. Med.* 296: 266-271, 1977

SPIGELMAN, I., SHANG, L. AND CARLEN, P.L. Patch-clamp study of postnatal development of CA1 neurons in rat hippocampal slices: membrane excitability and K^{+} currents. *J. Neurophsyiol.* 68(1): 55-69, 1992

STERIADE, M., JONES, E.G. AND MCCORMICK, D.A. Thalamus, *Elsevier Science*, 1997

SULAIMAN, M.R. AND DUTIA, M.B. Opioid inhibition of rat medial vestibular nucleus neurones in vitro and its dependence on age. *Exp. Brain Res.* 122: 196-202, 1998

SULAIMAN, M.R., NIKLASSON, M. THANK, R. AND DUTIA, M.B. Modulation of vestibular function by nociceptin/orphanin FQ: an in vivo and in vitro study. *Brain Res.* 828(1-2): 74-82, 1999

SVOBODA, K.R. AND LUPICA, C.R. Opioid inhibition of hippocampal interneurons via modulation of potassium and hyperpolarization-activated cation (I_h) currents. *J. Neurosci.* 18(8): 7084-7098, 1998

SYKOVA, E., HAJEK, I., CHVATAL, A., KRIZ, N. AND DIATCHKOVA, G.I. Changes in extracellular potassium accumulation produced by opioids and naloxone in frog spinal cord: relation to changes of Na-K pump activity. *Neurosci Lett* 59(3): 285-290, 1985

TANG, T., STEVENS, B.A. AND COX, B.M. Opioid regulation of intracellular free calcium in cultured mouse dorsal root ganglion neurons. *J. Neurosci. Res.* 44(4): 338-343, 1996

TENNIGKEIT, F., SCHWARZ, D.W.F. AND PUIL, E. Mechanisms for signal transformation in lemniscal auditory thalamus. *J. Neurophysiol.* 76(6): 3597-3608, 1996

TENNIGKEIT, F., PUIL, E. AND SCHWARZ, D.W. F. Firing modes and membrane properties in lemniscal auditory thalamus. Acta Otolaryngol. 117(2): 254-257, 1997

TENNIGKEIT, F., SCHWARZ, D.W.F. AND PUIL, E. Postnatal development of signal generation in auditory thalamic neurons. *Dev. Brain Res.* 109: 255-263, 1998

TERENIUS, L. Stereospecific interaction between narcotic analgesics and a synaptic plasma membrane fraction of rat cerebral cortex. *Acta Pharmacol. Toxicol.* 32: 317-319, 1973

TOKIMASA, T., MORITA, K. AND NORTH, A. Opiates and clonidine prolong calcium-dependent after hyperpolarization. *Nature* 294: 162-163, 1981

UHL, G.R., CHILDERS, S. AND PASTERNAK, G. An opiate-receptor gene family reunion. *Trends Neurosci.* 17(3): 89-93, 1994

WANG, J.B., JOHNSON, P.S., PERSICO, A.M., HAWKINS, A.L., GRIFFIN, C.A. AND UHL, G.R. Human mu opiate repector. cDNA and genomic clones, pharmacologic characterization and chromosomal assignment. *FEBS Lett.* 338(2): 217-222, 1994

WILLIAMS, S.R., TURNER, J.P., ANDERSON, C.M. AND CRUNELLI, V. Electrophysiological and morphological properties of interneurones in the rat dorsal lateral geniculate nucleus *in vitro. J. Physiol.* 490(1): 129-147, 1996

WINER, J.A. AND LARUE, D.T. Anatomy of glutamic acid decarboxylase immunoreactive neurons and axons in the rat medial geniculate body. *J. Comp. Neurol.* 278: 47-68, 1988

YASUDA, K., RAYNOR, K., KONG, H. BREDER, C.D., TAKEDA, J., REISINE, T. AND BELL, G.I. Cloning and functional comparison of kappa and delta opioid receptors from mouse brain. *Proc.Natl. Acad. Sci. U.S.A.* 90(14): 6736-6740, 1993

ZHU, J., CHEN, C., XUE, J.C., KUNAPULI, S., DERIEL, J.K. AND LIU-CHEN, L.Y. Cloning of a human kappa opioid receptor from the brain. *Life Sci.* 56(9): PL201-207, 1995